sustainability

MDPI

Article

The Effect of a Liquified Wood Heavy Fraction on the Rheological Behaviour and Performance of Paving-Grade Bitumen

Vinicius Cordeiro [1], Margarida Sá-da-Costa [2,*], Carlos Alpiarça [3], José Neves [4], Rui Galhano dos Santos [5], João Bordado [5] and Rui Micaelo [6,*]

[1] Department of Civil Engineering, School of Science and Technology, Universidade NOVA de Lisboa, 2829-516 Caparica, Portugal; v.cordeiro@fct.unl.pt
[2] National Laboratory for Civil Engineering, 1700-111 Lisbon, Portugal
[3] LUSASFAL—Derivados Asfálticos de Portugal, S.A., 7080-341 Vendas Novas, Portugal; carlos@lusasfal.pt
[4] CERIS, Instituto Superior Técnico, Universidade de Lisboa, Avenida Rovisco Pais, 1049-001 Lisboa, Portugal; jose.manuel.neves@tecnico.ulisboa.pt
[5] CERENA, Instituto Superior Técnico, Universidade de Lisboa, Avenida Rovisco Pais, 1049-001 Lisboa, Portugal; rui.galhano@tecnico.ulisboa.pt (R.G.d.S.); jcbordado@ist.utl.pt (J.B.)
[6] CERIS, Department of Civil Engineering, School of Science and Technology, Universidade NOVA de Lisboa, 2829-516 Caparica, Portugal
* Correspondence: mcosta@lnec.pt (M.S.-d.-C.); ruilbm@fct.unl.pt (R.M.)

Abstract: Biomass is one the most abundant renewable energy sources, and it can be processed through different thermochemical methods to obtain oils that can replace the petroleum bitumen used in road construction. For the construction industry to accept the bitumen replacement with bio-oil, it is necessary to know its properties and determine the applicability of conventional testing methods. This research utilized a liquified wood heavy fraction (bio-oil) obtained from waste wood through an innovative thermochemical liquefaction process. The aim was to investigate a kind of bio-bitumen produced by blending this bio-oil with paving-grade bitumen. The rheological behaviour in a wide temperature range, the performance relative to fatigue cracking and permanent deformation sensitivity, and the evolution with oxidative ageing were evaluated for the bio-bitumen and paving-grade bitumens. The bio-oil significantly affected the rheological behaviour of bitumen through an overall decrease in the phase angle and by failing the time–temperature superposition principle. The strong elastic response of the bio-bitumen improved resistance to fatigue and permanent deformation accumulation; however, resistance to oxidative ageing declined. Linear viscoelastic rheological indicators proposed in the literature to assess the material's performance showed a similar trend of variation with oxidative ageing for bio-bitumen and paving-grade bitumen, though the indicators' values could not be directly compared.

Keywords: biomass; bio-bitumen; thermochemical conversion; rheological characterization; permanent deformation; fatigue; performance indicators

Citation: Cordeiro, V.; Sá-da-Costa, M.; Alpiarça, C.; Neves, J.; Galhano dos Santos, R.; Bordado, J.; Micaelo, R. The Effect of a Liquified Wood Heavy Fraction on the Rheological Behaviour and Performance of Paving-Grade Bitumen. *Sustainability* **2024**, *16*, 972. https://doi.org/10.3390/su16030972

Received: 15 December 2023
Revised: 8 January 2024
Accepted: 14 January 2024
Published: 23 January 2024

1. Introduction

The transportation network plays a central role in facilitating local economic growth, thereby contributing substantially to regional and national development. However, this vision remains unrealized in numerous medium- and low-income countries where substantial investments are still required to establish essential transport connections across diverse territories [1]. Conversely, high-income countries boast extensive networks supporting the mobility of people and goods through various modes of transportation; yet, they grapple with the challenge of ensuring sustainable, long-term serviceability. Simultaneously, the pressing need to combat the impacts of climate change is compelling global investments in technological solutions in the transportation sector, for both vehicles and infrastructure, aimed at reducing long-term emissions.

Relative to road transportation, in the next few decades, the most relevant transformation in vehicles will be the expansion of zero-emission vehicle fleets [2], which will also impact the way roads will be built and maintained. Most roads are currently paved with bituminous materials, a mixture of mineral aggregates and bitumen, with the latter constituent being a petroleum-derived product. Hence, the intended reduction in the global consumption of petroleum-based fuels will reduce petroleum-refined volumes [3] and, in the end, the availability at a reasonable cost of bitumen for the road construction industry.

Bitumen binds the variable-sized aggregate fractions that allow the formation of a cohesive and stable material under traffic, and, despite its low proportion in the mixture (4–7% in mass), it significantly affects production and on-site performance [4]. Thus, bitumen has complex mechanical and rheological behaviour that is strongly affected by temperature, showing solid-to-fluid behaviour only by the effect of temperature. In addition to that, bitumen's properties evolve with time (ageing), causing a global hardening and a decrease in flexibility as the result of oxidation reactions and other chemical reactions like, for example, polymerisation [5,6]. Hence, road pavements degrade with traffic and climatic actions, demanding frequent maintenance and rehabilitation actions during the service life. Although reclaimed bituminous materials from distressed road pavements can effectively be recycled [7], this process often requires the incorporation of virgin binders and rejuvenators. For these reasons, there is an important industrial interest in developing road paving binders from alternative sources to petroleum, namely, biomass [8,9].

Among the various renewable energy sources currently known, biomass has attracted the attention of researchers due to its low cost, plentiful availability and reduced environmental impact [10]. Biomass is treated through different physical and chemical processes to obtain products for different applications, namely, (bio-)oils that can eventually be a substitute for bitumen. The interest in this topic is confirmed by the research studies that have investigated the biomass treatment process and/or the bio-oil properties from different biomasses, such as sunflower shell, walnut shell, almond shell, hazelnut shell [11], pine tree [12], corncob, tea waste, beech wood [11], industrial wood waste [13], spruce wood, olive husk [11], coconut husk, sawdust [14], rapeseed oil [15,16], sunflower oil [16,17], plant residue [13], waste cooking oil [14,18–21], waste motor oil [22], soy oil residue, fish oil, algae and swine manure [23–25].

Often, biomass is classified relative to the source (woody plants and agricultural products, herbaceous plants, aquatic plants, and manure/waste) and the natural water content (low/high) [26]. The water content influences the biomass processing technique and the conditions adopted, though other factors, e.g., calorific value, ash residue content, cellulose/lignin ratio, etc., are also relevant to define the process. The main biomass processing methods are gasification, pyrolysis and liquefaction [24]; however, to the best knowledge of the authors, gasification has not been used to obtain oils for bitumen replacements. Pyrolysis consists of decomposing biomass in a heated environment (300–900 °C) without oxygen, i.e., converting biomass into smaller molecules by heat absorption, and it is classified as slow, intermediate or fast according to the heating rate and time of exposure [23]. Pyrolysis is particularly suitable for drier biomasses and, in the end, the bio-oil, which sums 70–80% of end-products, is composed of a complex mixture of oxygenated organic compounds, including alcohols, aldehydes, esters, saccharides, phenolic compounds, carboxylic acids and lignin oligomers [27]. Conversely, liquefaction decomposes biomass in a hot, liquid and pressurised environment, and different liquids (solvents) can be used (e.g., water, methanol, etc.) to treat different biomasses. Thus, the biomass does not require being dried beforehand. Using liquefaction in water (hydrothermal processing), a hydrocarbon-rich product (bio-crude) is obtained in the intermediate range of temperature and pressure conditions of 300–350 °C and 120–180 atm (high pressure is necessary to avoid water boiling) [28]. According to Machado et al. [29], in recent years, the thermochemical process of pyrolysis has been chosen over liquefaction, with the latter process being used in only 30% of studies; however, in most cases (70%) the bio-oil was further processed into fuel.

The bio-products obtained from pyrolysis and liquefaction have different properties related to the chemical compounds formed during biomass decomposition. Thus, pyrolysis oils usually have a significantly higher oxygen on water free basis than that of hydrothermal liquefaction products [24]. In addition, the chemical composition of the bio-products (oil or crude) obtained with the two processing methods changes with the biomass source and characteristics.

For the construction industry to accept a bitumen replacement, partial or full, with these bio-products, it is necessary to know their properties, especially the ones most valuable to road pavement construction and performance, such as rheological properties, adhesion to aggregates, cohesion, ductility, etc. Hence, as shown in Table 1, different studies have evaluated the mixture of bio-oil and bitumen in the laboratory. Often, the proportion of bio-oil substitution is small (<10%) to ensure that the physical and rheological properties of the bio-bitumen are similar to those of conventional bitumen, i.e., as the bio-oil viscosity is usually much lower than that of bitumen, the oil content is reduced to obtain a satisfactory bitumen consistency for road service conditions. Based on the oil substitution proportion, the process can be categorised as a bitumen modifier, in which the replacement of bitumen is less than 10%; a bitumen extender, where bio-oil is used between 20% and 75%; or a direct alternative binder, where the replacement of bitumen is total (100%) [30].

Recent reviews that discuss in more detail the biomass thermochemical processes to obtain bio-oil for road construction and the properties of bio-bitumen and bio-asphalt can be found in [23,24,31,32]. These reviews point out that in comparison with base bitumen, the performance of bio-bitumen can be better or worse in different temperature ranges (low, intermediate and high), and the same occurs for bituminous mixtures. Ameri et al. [31] showed that there is high variation among bio-oils from the same biomass source processed with different methods and that there are no established methods for evaluating and comparing the performance of bio-bitumens. Bio-oils have different chemical compounds from bitumen, and the interaction between them can increase or decrease the mobility of molecular chains at different temperatures, which affects resistance to thermal- and fatigue-cracking and rutting [32]. Some bio-oils increase the polarity of the binder and can contain hydrophilic compounds, changing the hydrophobic characteristic of bitumen to hydrolytic, and these effects can facilitate the moisture damage of bituminous mixtures [31]. In addition, it was found that bio-oils with high polar compounds have increased sensitivity to oxidation, whereas phenolic compounds act as anti-ageing agents [31].

Bio-bitumens can be a more sustainable solution than petroleum bitumen. The association Eurobitume estimated a current environmental impact of 207.5 kg CO_2 eq to produce 1 tonne of bitumen, which includes crude oil production, transportation, refining, storage and the required infrastructure [33]. Samieadel et al. [34] conducted a comparison of greenhouse gas emissions between bitumen and bio-bitumen derived from swine manure oil. They reported a significant reduction in methane, carbon dioxide, and nitrous oxide emissions for the bio-bitumen. This environmental benefit is particularly pronounced when using waste biomasses that might otherwise end up in landfills. In their study, the authors [34] highlighted a reduction of over 80% in gas emissions by converting swine manure to bio-oil compared to storing it in a lagoon.

Table 1. Production parameters of different bio-oils.

Type of Bio-Oil	Source	Bio-Oil Proportion (w %)	Base Bitumen	Bio-Binder Penetration (0.1 mm)	Study
Wood oil	Industrial waste [18]	0.5, 10, 15	Bitumen 50/70	71.3, 114.4, 153.5	Laboratory test
	Pine tree [12]	100	Bitumen 30/45	21	Laboratory test
	Pine tree [35]	1, 5, 10	Bitumen 35/50	35–45, 35–85, 20–150	Laboratory test
	Kraft lignin powder [36]	5, 10, 15	Bitumen 50/70	57, 51, 42	Laboratory test
	Industrial waste (eucalyptus) [13]	5, 10, 20, 40, 60	Bitumen 50/70	79, 108, 97, 136, 168	Laboratory test
	Industrial waste (hardboard) [37]	5, 10, 20, 40	Bitumen 50/70	48–52, 45–50, 44–46, 42–45	Laboratory test
Vegetable oil	Not disclosed [38]	10	Bitumen 60/70	50–60	Laboratory test
	Rapeseed [15]	7.5, 8.0	Bitumen 160/220	-	Surface dressing of roads in Iceland
	Rapeseed [16]	18	Bitumen 15/25	33.7	Laboratory test
	Sunflower [16]	18	Bitumen 15/25	44.9	Laboratory test
	Sunflower [17]	2, 4, 6, 8, 10	Bitumen 70/100	80–90, 90–100, 160–170, 180–200, 240–260	Laboratory test
Animal oil	Fish [15]	7.0	Bitumen 160/220	-	Surface dressing of roads in Iceland
	Swine manure [18]	5, 10, 15	Bitumen 50/70	71.3, 114.4, 153.5	Laboratory test
Waste cooking oil	Not disclosed [20]	3, 4, 5	Bitumen 60/70	99, 136, 153	Laboratory test
	Not disclosed [39]	5, 10, 15	Bitumen 60/70	50–60, 60–70, 70–80	Laboratory test
	Not disclosed [19]	0.5, 1.0, 1.5, 2.0, 2.5, 3.0	Bitumen 50/70	33–38, 40–45, 45–50, 57–60, 58–62, 62–65	Laboratory test
	Not disclosed [40]	2, 4, 6, 8	Bitumen 40/60	60–70, 80–95, 125–135, 185–195	Laboratory test
	Not disclosed [21]	1, 2, 3, 4, 5	Bitumen 80/100	50–55, 70–75, 80–85, 95–100, 130–135	Laboratory test
Waste motor oil	Not disclosed [22]	10	Bitumen 35/50	114	Laboratory test

2. Objectives and Scope

The main goal of this study was to assess the potential of a new kind of bio-based bitumen—bio-bitumen—that incorporates a liquified wood heavy fraction extracted from waste wood through an innovative thermochemical liquefaction process [29,41] to be used in bituminous mixtures. This was accomplished by characterising its rheological behaviour in a wide temperature range, performance relative to fatigue cracking and permanent deformation sensitivity, and evolution with oxidative ageing. In addition, this study analysed the applicability to the studied bio-bitumen of some linear viscoelastic rheological performance indicators proposed in the literature for conventional bitumens.

The liquified wood heavy fraction (bio-oil) was blended with conventional bitumen to obtain a bio-bitumen with the same consistency at intermediate temperatures as the most-used bitumen in the country (35/50 grade). This study was conducted as part of the "BioRoadPAV®—New Bio-Binders for Application in Road Pavements" project (2021–2023), aiming to develop bio-binders derived from bio-oils sourced from biomass materials (waste wood) [42].

3. Materials and Methods

3.1. Materials

Two bitumens (B10/20 and B35/50) and one bio-bitumen were used in this study. The hard-paving-grade bitumen B10/20 (penetration 10–20 $\times$ 10^{-1} mm) was blended with a liquified wood heavy fraction (bio-oil) to obtain a bio-bitumen with a penetration within the grade of 35/50 bitumen. A commonly used paving-grade bitumen, B35/50 (penetration 35–50 $\times$ 10^{-1} mm), served as the reference material in the investigation of the bio-bitumen. The bio-bitumen and reference bitumen were studied in both unaged and (short-)aged states, being the aged materials referred to in the text as Bio-A and B35/50-A, respectively. The ageing procedure was the rolling thin film oven test (RTFOT), EN 12607-1 [43]

The wood biomass was converted into a bio-oil through direct liquefaction (thermochemical) by a catalytic depolymerisation process that occurred at atmospheric pressure in the presence of an acid catalyst and that did not require the drying of the biomass. In the literature [24], the successful implementation of thermochemical liquefaction with different types of biomasses is described. In this study, the biomass used was composed of wood residues (pinewood) resulting from systematic cleaning interventions in forested areas or post-fire situations. The bio-oil was produced within the BioRoadPAV® project with a new patented process (European Patent EP 3689 847 A1) based on thermochemical liquefaction in the presence of an acid catalyst and a solvent. In this process, the simultaneous depolymerisation of the different wood structures (lignin, cellulose and hemicellulose) present in the raw material occurs [41]. The wood waste was transformed into an oil that was further processed, firstly by washing it with water to remove the components rich in oxygen—mainly sugars originated by the depolymerisation of the wood structures—and, afterwards, it was vacuum-distilled in a rotary evaporator to remove the low molecular weight compounds. The final product (liquified wood heavy fraction) was a highly viscous material composed of a mixture of branched polymers with contents of PAHs (polycyclic aromatic hydrocarbons) hundreds to thousands of times lower than those of bitumen derived from crude oil. The reagents used were 2-ethylhexanol (purity $\geq$ 99%, technical grade) and p-toluenesulfonic acid (PTSA, purity $\geq$ 99%, technical grade) from a local supplier.

The bio-oil was characterized by FTIR-ATR (Fourier transform infrared spectroscopy—attenuated total reflectance) to analyse its chemical composition in terms of main functional groups and compare it with those detected in the paving-grade bitumens. Figure 1 shows the spectra of the oil and of B35/50. The comparison of the two spectra indicates major differences between the bio-oil and the bitumen composition associated with the presence of oxygen in the molecular structures, i.e., the bio-oil had a relevant proportion of functional groups containing oxygen, contrary to the bitumen, the presence of which was not detected in the spectrum. In the spectrum of the first one, the presence of hydroxyl (OH) groups of alcohols was detected due to the broad band at 3600–3200 cm^{-1}, and oxidated groups with carbonyl bond (C=O) were detected due to the strong band at 1727 cm^{-1} of C=O stretching, which can be associated with esters, aldehydes, ketones and carboxylic acids. Absorption bands in the range of 1300–1000 cm^{-1}, assignable to the stretching of the C-O of ethers, esters and hydroxyl groups, were also detected.

Additionally, the bio-oil was subjected to a thermogravimetric analysis (TGA) in a nitrogen environment within the temperature range of 25–800 °C [42]. The TGA results revealed a total mass loss of 81%, with the peak mass loss rate occurring at 160 °C. Consequently, within the intended application temperature range (<200 °C), the bio-oil sample experienced a 37% loss of its mass. It is noteworthy that the bio-oil composition included a substantial distillable fraction, which was lost due to the influence of temperature.

The content of bio-oil that could be incorporated in the bitumen was defined based on conventional consistency tests for bitumens, i.e., needle penetration at 25 °C (EN 1426 [44]) and the softening point/ring and ball method (EN 1427 [45]). Table 2 compares the consistency of the two bitumens and the bio-oil based. The penetration value of the bio-oil was very high, meaning that it was softer than the bitumens at room temperature. However, the softening point was also very high, which meant that the bio-oil was less deformable at

high temperatures than the other bituminous materials. From this, the bio-oil was blended with the hard-grade bitumen (B10/20), using two proportions in the mixture (15% and 20% by weight of the final mixture). To produce the bio-bitumen, first, the materials were heated (190 °C for bio-oil and 150 °C for bitumen) in a ventilated oven for 45 min and then the bio-oil was added to the bitumen. The mixtures were first homogenised by hand with a glass rod and then with a mechanical stirrer at 1650 rpm for 20 min. The temperature was kept between 170 °C and 180 °C during the agitation period. Figure 2 shows the aspect of the bio-oil and the bio-bitumen in a penetration test container. The penetration value of the bio-bitumens was 52 × 10^{-1} mm and 40 × 10^{-1} mm for the mixtures with 20% and 15% of bio-oil, respectively. Considering the initial objective of studying a bio-bitumen with a similar consistency to that of the most-used paving-grade bitumen, which, in southern European countries, is grade 35/50, the bio-bitumen with 15% wood-based bio-oil was selected to continue the research. Thus, as shown in Table 1, this level of bio-oil incorporation is in line with current practice.

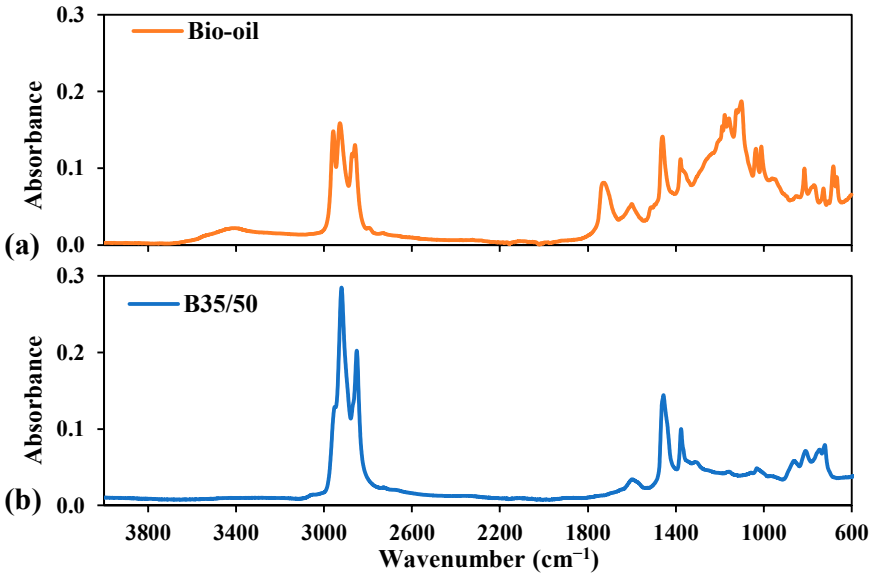

Figure 1. FTIR-ATR spectra: (**a**) bio-oil; (**b**) bitumen (B35/50).

Table 2. Consistency properties of the bitumens and bio-oil.

Property	Test Method	B10/20	B35/50	Bio-Oil
Penetration @25 °C (0.1 mm)	EN 1426	17	43	213
Softening point (°C)	EN 1427	65.0	53.0	112.5

(**a**) (**b**)

Figure 2. Surface image of samples: (**a**) bio-oil; (**b**) bio-bitumen.

3.2. Linear Viscoelastic Rheological Characterisation

The linear viscoelastic (LVE) behaviour of the different bituminous binders was characterised under dynamic oscillatory testing using a parallel plates setup. The rheological functions considered were the norm of the complex shear modulus ($|G^*|$) and the phase angle (δ) over a defined range of frequencies and temperatures. The equipment used was the SmartPave (Anton Paar) rheometer equipped with a Peltier system to control the specimen temperature. The test procedure generally followed the European standard EN 14770:2012 [46]. A frequency sweep test from 0.1 rad/s to 100 rad/s was performed at temperatures from −30 °C to 82 °C with 6 °C steps, which allowed for the characterisation of the rheological viscoelasticity of the materials from the near-glassy behaviour up to a state dominated by the viscous component. Given the wide range of temperatures and the samples' stiffness, three plate sizes (diameters) were used (4 mm, 8 mm and 25 mm). The 4 mm diameter plates with a 1.75 mm gap were adopted from −30 °C to 10 °C, the 8 mm diameter plates with a 2 mm gap were used from −6 °C to 40 °C and the 25 mm diameter plates with a 1 mm gap were used from 28 °C to 82 °C. The highest temperature limit for Bio-A was increased up to 106 °C because of its consistency. An overlap of two or three temperatures was performed with the 4 mm and 8 mm plates and with the 8 mm and 25 mm plates to ensure that adequate measurements, i.e., within the compliance limits of the equipment and test geometry, were obtained for all tested materials. To ensure that materials were tested in the linear viscoelastic region (LVR), previous strain sweep tests from 0.001% to 10% at the two extreme frequencies (0.1 rad/s and 100 rad/s) were performed at the lowest and highest test temperature for each plate diameter. The strain amplitude ranges selected for the different materials were 0.001–0.003%, 0.010–0.100% and 0.100–0.500% for the geometries of 4 mm, 8 mm and 25 mm, respectively.

3.3. Multiple Stress Creep and Recovery Test

The multiple stress creep and recovery test (MSCRT) was carried out based on EN 16659 [47] to characterise the susceptibility of the material to accumulating permanent deformation. The test procedure was implemented in the rheometer with parallel plates of 25 mm with a gap of 1 mm at 60 °C. The test consisted of subjecting the disc-shaped specimen to 20 cycles of shear loading for 1 s and a rest period of 9 s. The load applied was 0.1 kPa for the first 10 cycles and 3.2 kPa for the other 10 cycles. At least two specimens were tested for each material. During the test, the shear strain was monitored to determine the percentage of recovery ($\%R$) and the non-recoverable creep compliance (J_{nr}). The $\%R$ value in cycle N ($\%R^N$) was calculated as follows:

$$\%R^N = \frac{100 \cdot \left(\varepsilon_1^N - \varepsilon_{10}^N\right)}{\varepsilon_1^N} \quad (1)$$

in which ε_1^N is the strain value after 1 s (end of loading) and ε_{10}^N is the strain value after 10 s (end of the rest period). The individual values of $\%R^N$ determined the average value of the percentage recovery at each stress level ($\%R_\tau$) and the value of R_{diff} indicated the effect of the stress level on the material response, as follows:

$$\%R_\tau = \frac{1}{10}\sum_{N=1}^{10} \%R_\tau^N \quad (2)$$

$$R_{diff} = 100 \cdot \frac{\left(\%R_{0.1\text{kPa}} - \%R_{3.2\text{kPa}}\right)}{\%R_{0.1\text{kPa}}} \quad (3)$$

The non-recoverable creep compliance at cycle N and at stress level τ (kPa) ($J_{nr\,\tau}^N$) was calculated as follows:

$$J_{nr\,\tau}^N = \frac{\varepsilon_{10}^N}{\tau} \quad (4)$$

Similarly to the percentage recovery, the J_{nr}^{N} values were averaged at each stress level and the quantity $J_{nr\text{-}diff}$ was determined as follows:

$$J_{nr\ \tau} = \frac{1}{10}\sum_{N=1}^{10} J_{nr\ \tau}^{N} \quad (5)$$

$$J_{nr-diff} = 100 \cdot \frac{(J_{nr\ 3.2\text{kPa}} - J_{nr\ 0.1\text{kPa}})}{J_{nr\ 0.1\text{kPa}}} \quad (6)$$

3.4. Fatigue Resistance–Linear Amplitude Sweep Test

To evaluate the fatigue behaviour of the bitumens, the linear amplitude sweep (LAS) test defined in AASHTO T 391-20 was adopted [48]. This is an oscillatory test in which the shear strain amplitude is progressively (linearly) increased. The test was conducted in a rheometer with a parallel plate setup. Plates with a diameter of 8 mm and a 2 mm gap were used and 100 cycles were applied at every strain level (frequency of 10 Hz). In this study, the temperature of 20 °C was adopted, which is representative of intermediate conditions in-service. During the test, stress and strain were monitored to calculate the shear modulus and phase angle.

The LAS test results were then processed based on viscoelastic continuum damage (VECD) mechanics to determine the material's fatigue law:

$$N_f = A \cdot \gamma^{-B} \quad (7)$$

where N_f is the number of cycles to failure, γ is the strain amplitude and A and B are material constants. In this study, the procedure described by Carl et al. [49] was used, which uses the pseudo-strain energy density to quantify work and adopts the constant α, as follows:

$$\alpha = 1 + \frac{1}{m} \quad (8)$$

where m is the maximum slope of the logarithm values of the storage shear modulus versus the angular frequency. To determine the m value, the cyclic damage test was preceded by a frequency sweep test in linear viscoelastic conditions (0.1% strain, 0.2–30 Hz). Additional information relative to the VECD mechanisms and the methods used to analyse the LAS results can be found in the literature [49–51].

3.5. LVE Rheological-Based Performance Indicators

The importance of an accurate rheological and mechanical characterisation of bituminous materials has been acknowledged by the scientific and technical community at least since the development of the Strategic Highway Research Program (SHRP) [52] in the USA from 1987 to 1993, which resulted in the Superpave performance-based specifications (PG system). From this research, the PG system adopted criteria (maximum/minimum values) for some rheological measurements of the bitumens that were related to the most expressive distresses in asphalt pavements (thermal cracking, fatigue cracking and rutting) [53]. The thermal cracking performance was related to the creep stiffness and the slope of the stiffness master curve, both obtained with a bending beam rheometer (BBR), and the fatigue cracking and rutting performance were related to the dynamic response obtained with a dynamic shear rheometer (DSR) in terms of the $|G^*| \cdot \text{Sin}(\delta)$ and $|G^*|/\text{Sin}(\delta)$, respectively. Also, considering the expected evolution of the rheological behaviour with ageing, these criteria needed to be met at different ageing states (original, short- and/or long-term). However, since then, different research studies have reported the limitations of these criteria to avoid the poor field performance of some bitumens [54] or validate the enhanced performance of other bitumens (e.g., polymer-modified bitumens) [55]. Nevertheless, other studies have proposed different rheological-based indicators, which can be expected to be included in the next bitumen specifications, such as in the upcoming revisions of the European standards [56]. In addition, bitumens incorporating biomaterials

are non-conventional bituminous binders, and the proposed rheological indicators may not apply to them. From this, some relevant LVE rheological-based performance indicators that have been proposed and discussed in recent years were selected as the materials to be studied. The indicators selected were the following: glass transition temperature (T_g) and modulus ($|G^*|_g$); crossover temperature (T_c) and modulus ($|G^*|_c$); *R-value*; intermediate region temperature amplitude (ΔTIR); and temperature (T_{50kPa} and T_{5MPa}) and phase angle (δ_{50kPa} and δ_{5MPa}) of iso-moduli $|G^*| = 50$ kPa and $|G^*| = 5$ MPa.

Glass transition temperature is related to material performance in very cold weather, i.e., thermal cracking distress, and it can be determined with different test methods, including rheology [57]. Thus, based on polymer science, Elwardany et al. [58] investigated the use of the temperature at which the loss modulus is the maximum, as a substitute of T_g determined from differential scanning calorimetry, and concluded that the two methods correlated well. Although bituminous binders have an almost constant glass shear modulus of 1 GPa, irrespective of the origin and ageing state [5], to provide a detailed characterisation of the studied materials, the modulus at T_g was also determined. An increase in T_g was expected with ageing [57] and the opposite variation was expected with softening agents (e.g., oils) [59].

The crossover point corresponds to the transition—with increasing temperatures—from elastic dominant behaviour ($\delta < 45°$) to viscous dominant behaviour ($\delta > 45°$), and it is claimed to mark the high-temperature limit of the intermediate region in bitumen rheological behaviour [58]. The other regions—below and above the intermediate region—are the glassy region and the terminal region, respectively. Hence, the temperature intermediate region amplitude ΔTIR is the difference between T_g and T_c. Also, the logarithm difference between $|G^*|_c$ and $|G^*|_g$, known as the *R-value*, has also been related to bitumen fatigue performance [57]. Due to the effect of ageing, previous research [60] reported an increase of T_c and a decrease of $|G^*|_g$, which then leads to an increase in the *R-value*.

The other indicators correspond to two stiffness levels ($|G^*| = 50$ kPa and $|G^*| = 5$ MPa) that have been intensively discussed regarding their inclusion in the revisions of the European standards for bituminous binders, despite them requiring for now only the reporting of test values. The temperature at the highest stiffness (5 MPa) is aimed at giving an indication of fatigue cracking performance so that the lower the temperature is, the better the expected performance [56]. In opposition, the higher the temperature for the lower stiffness level (50 kPa), the better the expected performance for rutting resistance [56]. Besides the iso-stiffness temperatures, the phase angles have also been determined. Both temperatures are expected to increase with the hardening of bitumen caused by the ageing process, and the opposite trend is expected for the phase angles.

In previous studies, e.g., [57,58,61], several of these indicators were determined from the master curves of the shear modulus and phase angle versus the reduced frequency or reduced temperature; however, as shown in Section 4.2, bio-bitumen is not a thermo-rheologically simple material. Hence, in this study, all indicators were determined from the isochrone curves of the shear modulus and phase angle obtained in the LVE range at the frequency of 10 rad/s. This loading frequency is the same used to determine the $|G^*| \cdot \mathrm{Sin}(\delta)$ and $|G^*|/\mathrm{Sin}(\delta)$ values in the PG bitumen specifications and in the draft versions of the upcoming European standards. Although the isochrone curves could be obtained from the data obtained in frequency sweep tests at different temperatures, a single frequency test (10 rad/s) was conducted for the complete temperature range, considering 15 measurement points and 20 min for stabilisation at each testing temperature. Figure 3a,b compare, respectively, the $|G^*|$ and δ values obtained in the single frequency test and frequency sweep test for the tested materials (B10/20, B35/50, B35/50-A, Bio and Bio-A). The test results were nearly identical for all temperatures, which demonstrates that the frequency sweep test at different temperatures was sufficient to obtain a complete LVE rheological characterisation.

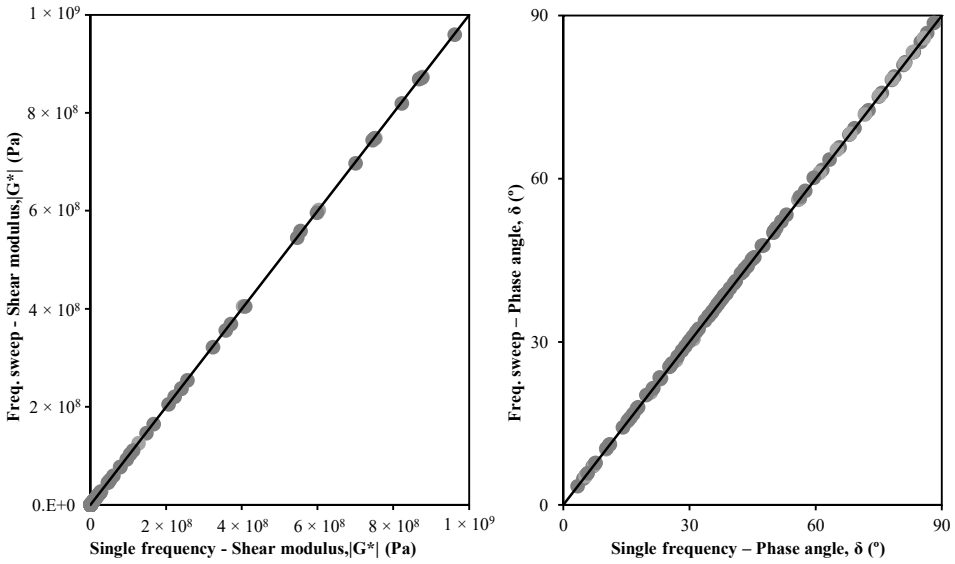

(**a**) (**b**)

Figure 3. Comparison of single-frequency and frequency sweep test results at 10 rad/s (all test data): (**a**) norm of the complex shear modulus; (**b**) phase angle.

Table 3 summarises the LVE rheological performance parameters that were selected and Figure 4 illustrates their determination from the isochrone curves of the complex shear modulus and phase angle at 10 rad/s of bitumen B35/50.

Table 3. LVE rheological-based performance indicators.

Performance Indicator	Variables	Method	Performance Indication	Expected Evolution with Ageing	
Glass transition point: temperature and modulus	T_g $\lvert G^* \rvert_g$	Peak in isochrone G'' at 10 rad/s	Thermal cracking	T_g $\lvert G^* \rvert_g$	↗ ~
Crossover point: temperature and modulus	T_c $\lvert G^* \rvert_c$	$\Delta = 45°$ in isochrone $\lvert G^* \rvert$ at 10 rad/s	Fatigue cracking	T_c $\lvert G^* \rvert_c$	↗ ↘
Intermediate region amplitude: temperature and modulus	ΔT_{IR} R-value	$\Delta T_{IR} = T_c - T_g$ $R = \log\lvert G^* \rvert_g - \log\lvert G^* \rvert_c$	Fatigue cracking	ΔT_{IR} R-value	↗ ↗
Point at high stiffness level $\lvert G^* \rvert$ = 5 MPa: temperature and phase angle	$T_{5\text{MPa}}$ $\delta_{5\text{MPa}}$	$\lvert G^* \rvert$ = 5 MPa in isochrone at 10 rad/s	Fatigue cracking	$T_{5\text{MPa}}$ $\delta_{5\text{MPa}}$	↗ ↘
Point at low stiffness level $\lvert G^* \rvert$ = 50 kPa: temperature and phase angle	$T_{50\text{kPa}}$ $\delta_{50\text{kPa}}$	$\lvert G^* \rvert$ = 50 kPa in isochrone at 10 rad/s	Permanent deformation	$T_{50\text{kPa}}$ $\delta_{50\text{kPa}}$	↗ ↘

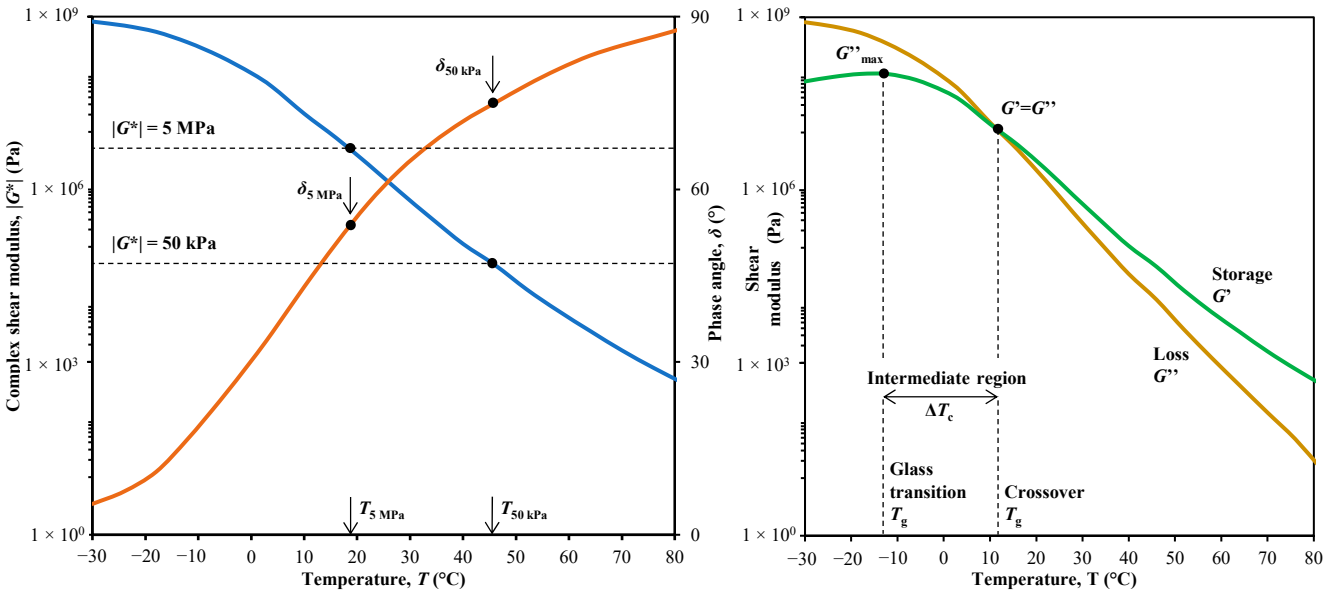

Figure 4. Illustration of the LVE rheological-based performance indicators for bitumen B35/50: (**a**) $|G^*|$ and δ vs. T; (**b**) G' and G'' vs. T.

4. Results and Discussion

4.1. Consistency Properties

The penetration and softening points of the bituminous binders, unaged and short-term aged, are presented in Table 4. In the unaged state, the bio-bitumen with 15% bio-oil had a similar penetration value to the B35/50; however, the softening point was much higher (11.4 °C). EN 13108-1 [62] indicates that the penetration or softening point of the binder of a mixture when reclaimed asphalt is used can be estimated simply by proportionally weighing the two binders. Adopting the same rule for the mixture of bio-oil and bitumen, Figure 5 shows that the softening point can be predicted well using the proposed rule; however, the penetration is significantly under-predicted.

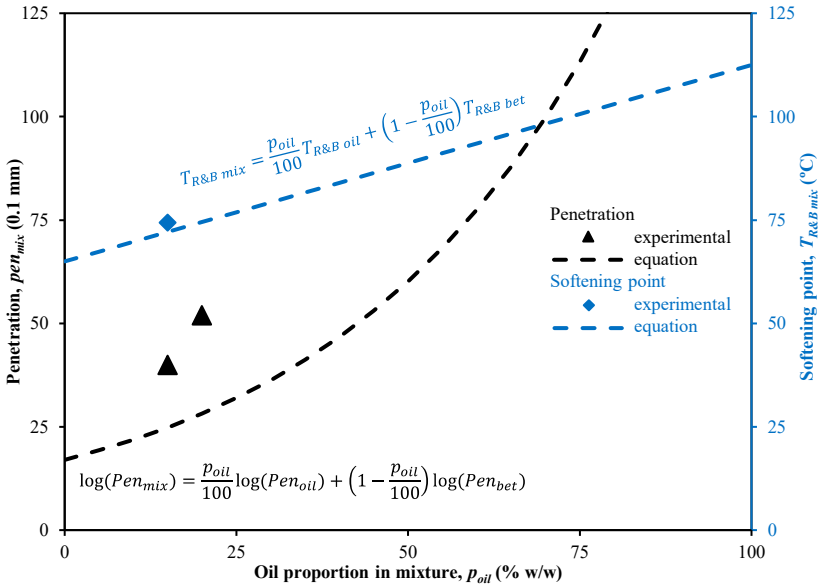

Figure 5. Experimental and predicted (EN 13108-1 [62] equations) values for penetration and softening points.

The penetration index, which measures the effect of temperature on the consistency, increased from 0 (B10/20) to +3 with the incorporation of 15% of bio-oil. This very low-temperature susceptibility is typical of polymer-modified bitumens in which the polymer chains provide a new structure to the bitumen, resulting in a decrease in deformability at high temperatures [63]. However, the bio-bitumen was significantly affected by the oxidative ageing induced in the rolling thin film oven test. The penetration value decreased to 31% of the initial value and the softening point increased by 27.1 °C, which exceeded for both tests the limits in the European specifications for paving-grade bitumens (EN 12591 [64]). Conversely, B35/50-A showed variation within the specification limits.

Table 4. Consistency properties of bituminous samples.

Property	Limits	B10/20	B35/50	B35/50-A	Bio	Bio-A
Penetration @25 °C (0.1 mm)	10–20 (1) 35–50 (2)	17	43	31	42	13
Softening point (°C)	60–76 (1) 50–58 (2)	65.0	53.0	59.2	74.4	101.5
Penetration index	−1.5 to +0.7 (2)	0	−0.8	−0.2	+3.1	+3.8
Retained penetration (%)	≥53% (2)	-	72		31	
Increase in softening point (°C)	≤11 °C (2)	-	6.2		27.1	

Notes: (1) limits for bitumen 10/20 (EN 13924-1 [65]); (2) limits for bitumen 35/50 (EN 12591).

4.2. Linear Viscoelastic Rheological Properties

The Black curves of the complex shear modulus versus the phase angle shown in Figure 6 provide, for the five binders, a general view of the rheological behaviour within the linear viscoelastic region. Under these conditions, paving-grade bitumens are usually "thermo-rheologically simple" materials, which means the rheological properties ($|G^*|$ and δ) are only dependent on temperature and time, and master curves can be generated by applying simple shift factors (time–temperature superposition principle, TTSP) [66]. Thus, the Black curve of a "thermo-rheologically simple" material should exhibit a smooth continuous variation between $|G^*|$ and δ, which the unaged bitumens B10/20 and B35/50 and RTFOT-aged B35/50-A were seen to follow. These bitumens presented single-curvature curves, showing the continuous decrease of $|G^*|$ with increasing δ that results from a certain overlap and continuity of the values obtained at different temperatures and frequencies. At very low temperatures, the complex shear modulus approached the value of 1 GPa, with a very small phase angle (<5°), whereas, at high temperatures, the modulus was close to null and the phase angle was 90°. Similar results have been reported before [67,68].

Conversely, the Black curves of the unaged and aged bio-bitumens had three distinct features that differentiated them from the paving-grade bitumens. Firstly, with the exception of the very high $|G^*|$ values obtained near the glassy state, the δ values of bio-bitumen were much lower than those of the bitumens for the same $|G^*|$ value, indicating a greater proportion of elastic behaviour. The second feature was the global trend of $|G^*|$ versus δ exhibiting double curvature, with a concave curve in the middle of two convex curves. The middle section—representing behaviour at the intermediate range of testing temperatures—had a steep slope, meaning that the $|G^*|$ value varied significantly with a small change in the phase angle. The third feature was the discontinuity in the intermediate part of the curve that was caused by measurements obtained at consecutive temperatures only overlapping for low test frequencies. In the literature [66], the partial discontinuity or branching in the Black curves has been attributed to different testing and material factors, such as testing outside of the linear viscoelastic region, compliance errors of the testing equipment and/or structural changes in the material during testing. Since the deformation applied with different geometries was determined from deformation sweep tests at different temperatures to ensure that it was within the linear viscoelastic region and that the rheometer was used within the normal working limits, this complex rheological behaviour

of bio-bitumen can be attributed to structural changes with the changes in temperature. Thus, Eckmann et al. [69] reported a similar type of "branching" in the Black curve of bitumen with a GEL-type structure, and they also concluded that the more structured the bitumen, the higher the phase angle is for the same given stiffness. Airey [66] found that bitumen modification with an EVA (ethylene vinyl acetate) polymer could create a strong discontinuity in the Black curve, which was explained by the somewhat changed crystalline structures in the material with changes in temperature. The strong effect of the studied bio-oil was also different to that reported in other studies that investigated different types of wood-derived oils in bitumen. In [12,18,35], the bio-oils caused a content-related shift of the Black curve to the right and slightly downwards, with an increased curvature, but the curve maintained the global shape. However, refs. [12,18] shows that the experimental results obtained at different temperatures are not always fully aligned; the authors concluded that bitumens with a higher bio-oil content (>10%) had only partial thermo-rheological simple behaviour.

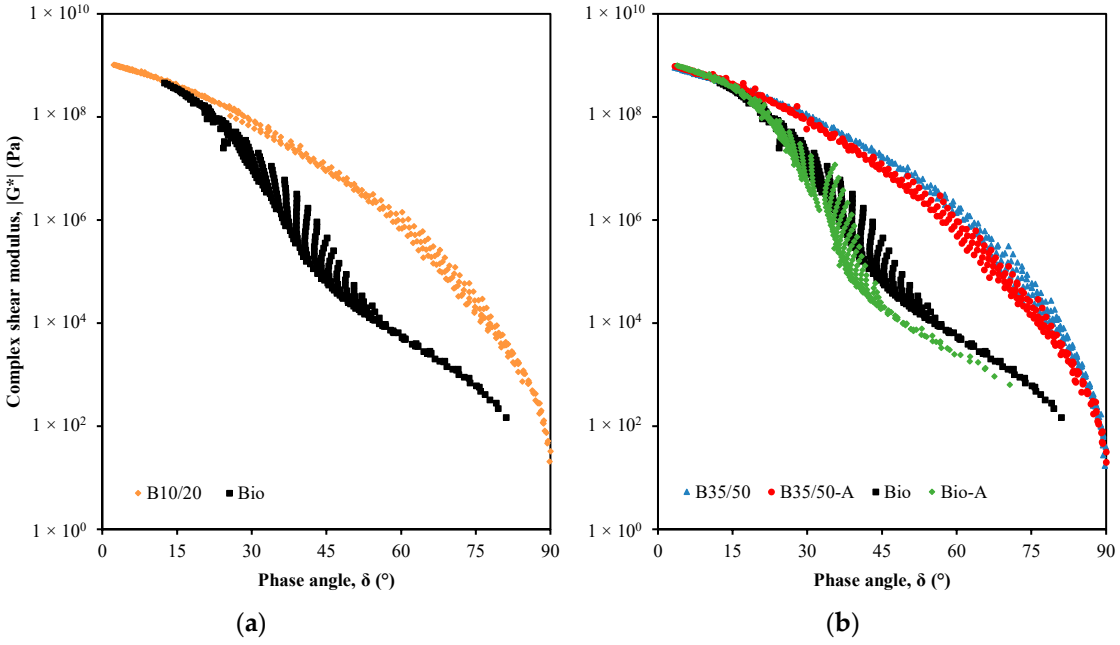

Figure 6. Black curves: (**a**) B10/20 and Bio; (**b**) B35/50, B35/50-A, Bio and Bio-A.

In addition, the RTFOT ageing treatment affected the Black curves. Similar to findings reported in previous studies [49,66,70], the curves moved to the left and slightly upwards, and these changes were more expressive in the bio-bitumen than in B35/50. However, as indicated by Airey [71], the increase in the complex shear modulus with ageing may not be perceptible from the Black curves because this effect occurs simultaneously with the decrease in the phase angle, and the resulting curves may be rather close together in the plot.

To further investigate the rheological behaviour of tested materials and analyse the effects of bio-oil and ageing, the isotherms of $|G^*|$ and δ at three temperatures (−18 °C, 22 °C and 64 °C) were plotted (see Figure 7) and Cole-Cole diagrams were drawn (see Figure 8).

The isotherms showed a clear increase along with the temperature in the variation of the rheological parameters among the materials. The amplitude of the variation in δ and the ratio of the $|G^*|$ values (max/min) for the different materials were approximately 10° and 6.2 at −18 °C, whereas, at 64 °C, these values were 49° and 1089. Thus, at 22 °C and 64 °C, the paving-grade bitumens (B10/20 and B35/59) had similar rheological behaviour, with the $|G^*|$ and δ values showing opposite trends (increase and decrease, respectively) with increasing frequency, and the stiffer the material was, the lower the phase angle

was, i.e., the material was less affected by viscous behaviour. Conversely, the unaged bio-bitumen showed a lower variation of $|G^*|$ with frequency at the various temperatures, and its δ values were significantly lower compared with the bitumens. Also, at 22 °C, the δ value was nearly constant with the frequency, which gave the nearly vertical "branches" seen in the middle part of the Black curve (see Figure 5). In addition, the effect of ageing treatment was very clear from the isotherms. Although the $|G^*|$ value increased and the δ value decreased with the ageing treatment for both materials, the magnitude of change was larger for the bio-bitumen, especially at the highest temperature (64 °C). Thus, it was observed that the aged bio-bitumen had largely elastic behaviour ($\delta < 45°$) over the range of temperatures represented (−18 to 64 °C), which was not anticipated.

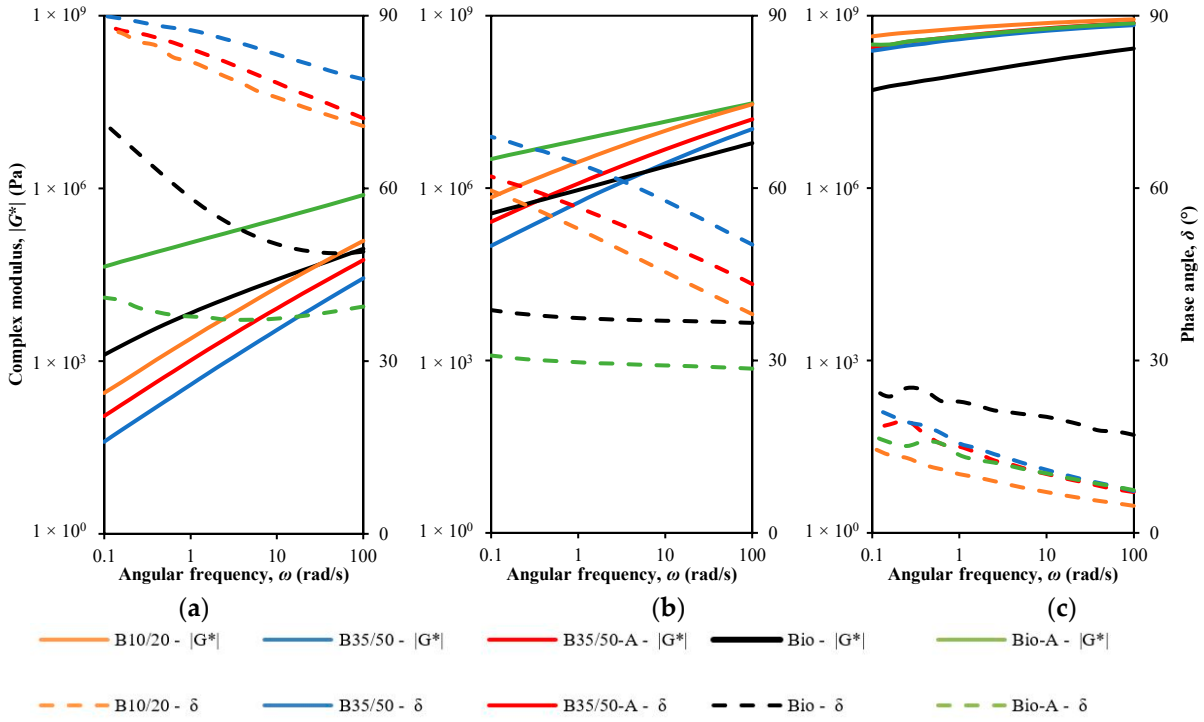

Figure 7. Isotherms of B35/50, B35/50-A, Bio and Bio-A at temperature (**a**) 64 °C, (**b**) 22 °C and (**c**) −18 °C.

From the Cole-Cole diagrams shown in Figure 8, it is possible to verify that B10/20 and B35/50 presented a similar balance between the viscous (loss), G'', and elastic (storage), G', components of the complex shear modulus, resulting in curves with a parabolic shape. It was also noted that the incorporation of the bio-oil changed the curve of the B10/20 both in shape and values. The two curves (B10/20 and Bio) were only coincident for the lowest values (highest test temperatures), and, by decreasing the temperature, the curve generally rotated clockwise, which corresponds to more elastic behaviour for a certain absolute shear modulus. Different from the paving-grade bitumens, the Bio curve did not show a peak marking the transition to the low-temperature zone, where the phase angle decrease is not compensated by the shear modulus increase. These changes in the Cole-Cole diagram are like those found with bitumen modification with SBS, which are more significant with increasing polymer content [72]. Also, the ageing treatment caused an expansion of the Cole-Cole diagram in the directions of both the x- and the y-axes, i.e., increases in the values of the storage modulus and loss modulus. It was observed, however, that Bio-A was more affected by the ageing treatment, approaching the usual behaviour of bitumen. The dispersion of measurements near the peak of the Cole-Cole diagrams, obtained at low temperatures with the 4 mm geometry, is also noteworthy. The test procedure with the 4 mm plate is not yet included in the European test standards and, in the literature [73], it

is reported that given the physical state of samples in this temperature zone, test results are very sensitive to the procedure of placing samples in the equipment, the time required for thermal and mechanical stabilisation before loading, and the loading amplitude applied. Thus, Bücher et al. [73] stated that the time required for a 4 mm sample stabilisation is longer than with other plates. Hence, based on [68,74], in this study, a time of 20 min was adopted with the 4 mm plate.

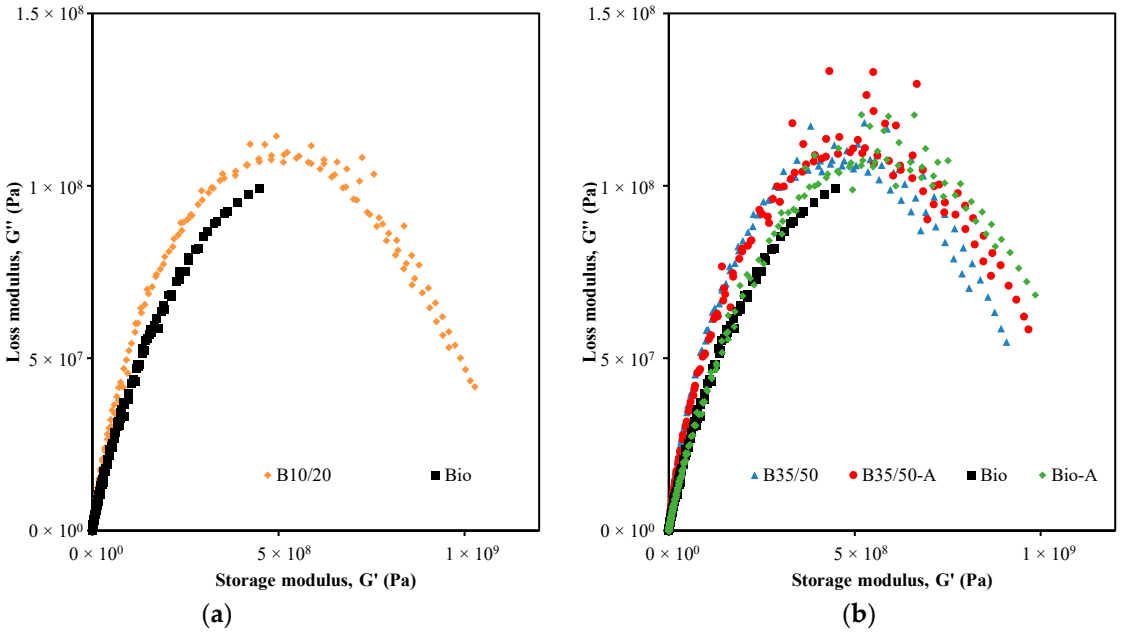

Figure 8. Cole-Cole diagrams: (**a**) B10/20 and Bio; (**b**) B35/50, B35/50-A, Bio and Bio-A.

4.3. Resistance to Permanent Deformation Accumulation

Previous studies found a strong correlation between the performance of the bitumen in the MSCR test and the accumulated deformation of bituminous mixtures [75], which is one of the most important types of distress in asphalt pavements. Thus, often, bio-oils have a lower viscosity than bituminous binders, which can lead to poor rutting resistance [8,76]. Table 5 summarises the results of the MSCR test at 60 °C for the studied binders. As expected, the hard-grade bitumen (B10/20) had greater elastic recovery and less non-recoverable compliance than the softer bitumen B35/50. For the load amplitude of 3.2 kPa, bitumen B35/50 had insignificant recovery (1.6%), which increased to 11% with the ageing treatment. The difference in values at 0.1 kPa and 3.2 kPa, especially those for %R, also demonstrates the significant stress dependence of these binders.

Table 5. MSCR test results.

Sample	Maximum Strain Average		%*R* (%)		R_{diff}	J_{nr} (kPa^{-1})		$J_{nr\text{-}diff}$
	0.1 kPa	3.2 kPa	0.1 kPa	3.2 kPa		0.1 kPa	3.2 kPa	
B10/20	0.029	0.969	21.8	19.1	12.5	0.228	0.240	5.0
B35/50	0.169	5.808	5.7	1.6	71.9	1.589	1.738	9.4
B35/50-A	0.060	2.021	16.9	11.0	34.6	0.502	0.548	9.3
Bio	0.012	0.400	71.0	64.7	8.8	0.034	0.044	28.3
Bio-A	0.001	0.027	93.2	93.4	−0.3	0.001	0.001	1.8

In opposition, the bio-oil greatly improved the test performance of bitumen B10/20. The elastic recovery value for Bio reached 71.0% at 0.1 kPa and the non-recoverable compliance decreased by approximately 82%. The effect of load amplitude on non-recoverable

compliance, quantified by $J_{nr\text{-}diff}$, was greater than that for the bitumens; however, as reported by [77], a small test value (%R or J_{nr}) often corresponds to high $J_{nr-diff}$ and $\%R_{diff}$ values. The performance of the bio-bitumen also improved with the ageing treatment in the creep test, in which the %R value attained 93.4% and J_{nr} was reduced to almost zero. The strain evolution in a single cycle at 3.2 kPa of the bitumens shown in Figure 9a demonstrated the change in the recovery properties with the bio-oil and ageing. The deformation recovery occurred very quickly after stress removal because the elastic component in the rheological behaviour of bio-bitumens is very strong.

The MSCR test performance in terms of both elastic recovery and non-recoverable compliance is often improved with polymer modification because this creates an active polymer structure that compensates for the elasticity that is lost when the bitumen's behaviour is mostly viscous [77,78]. Hence, the relation %R-J_{nr} in the MSCR test is used in materials specification AASHTO M 332 [79] to confirm the beneficial effect of polymer modification. Considering the good results of the bio-bitumens studied, in Figure 9b, the obtained test results are compared with the version of the AASHTO M 332 criterion modified by Anderson [80] to account for the lack of test results with J_{nr} values lower than 0.1 kPa^{-1} that were used to define the criterion. The results showed a clear separation of the performance rating for the bitumens and bio-bitumens. The bitumens fell below the curve, as expected for the unmodified (paving-grade) bitumens. The bio-bitumens were above the curve, meaning that their good performance in the MSCR test is in line with what can be expected for polymer-modified bitumens. In addition, following the specification of the high-temperature PG grade in AASHTO M 332 [79], which defines maximum J_{nr} values for RTFOT-aged binders, at the temperature of 60 °C (the temperature used herein), Bio is suitable for an extreme traffic level (>30 million ESALs), whereas B35/50 is only suitable for a lower traffic level (10–30 million ESALs).

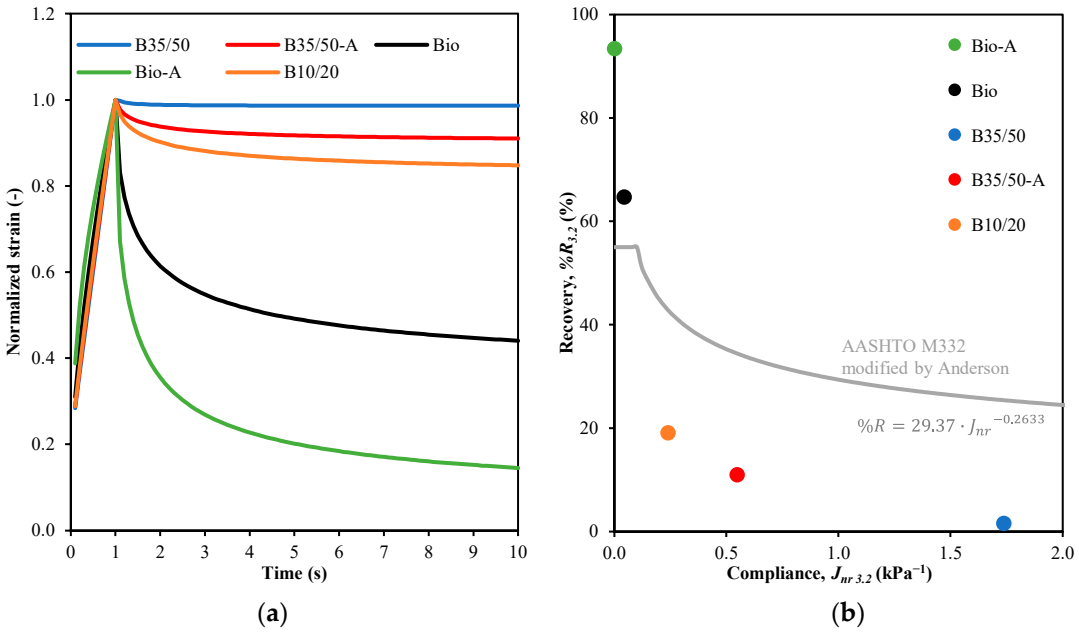

(**a**) (**b**)

Figure 9. MSCR test: (**a**) normalised strain evolution in the first cycle at 3.2 kPa; (**b**) relation $\%R_{3.2kPa}$-$J_{nr\ 3.2kPa}$ (AASHTO M332 equation modified by Anderson [78]).

4.4. Fatigue Resistance

The LAS test is a commonly used method to evaluate the (shear) fatigue behaviour of asphalt binders; it differs from the time sweep test because the load amplitude is increased throughout the process. For this reason, the LAS test takes less time and fewer samples are needed [81,82]. Regardless of the loading mode adopted, it is acknowledged that the cohesive failure of the disk-shaped specimen occurs due to the progression of radial

microcracks from the outer edge towards the centre of the specimen. In this study, the test was performed at 20 °C following the AASHTO T 391-20 standard, and the results were processed as described in [47]. Figure 10 presents the shear stress evolution with increasing applied strain and Figure 11 shows the fatigue laws for the tested materials. It was observed that the shear stress–strain curves of all tested materials were similarly shaped. The stress increased initially with the applied strain up to a certain point and then decreased quickly to a nearly constant small value. The curve peak marking the transition between the two regions was related to internal cracking and failure [51]; thus, it was used in the calculation procedure to obtain the fatigue laws. Due to the effect of the bio-oil, the bio-binder attained much smaller stress levels (20%) than the base bitumen B10/20 (Figure 10a); however, it was able to hold near-maximum stresses for a longer period, and failure was reached later (a strain of 10% vs. 5%) in the test. These differences were also valid for Bio and B35/50, though the stress level attained by the latter in comparison with the B10/20 was lower because it was a softer grade. Ageing treatment affected the binders' behaviour as expected, i.e., the stress levels increased and the strain at the peak stress decreased. However, the variation in Bio was much more intense than that in B35/50, which demonstrated the sensitivity of Bio to oxidative ageing. In the case of B35/50, the peak stress increased by 50% and the strain at peak stress decreased by 1%, whereas with Bio, the stress increased by 370% and the strain decreased by 5%.

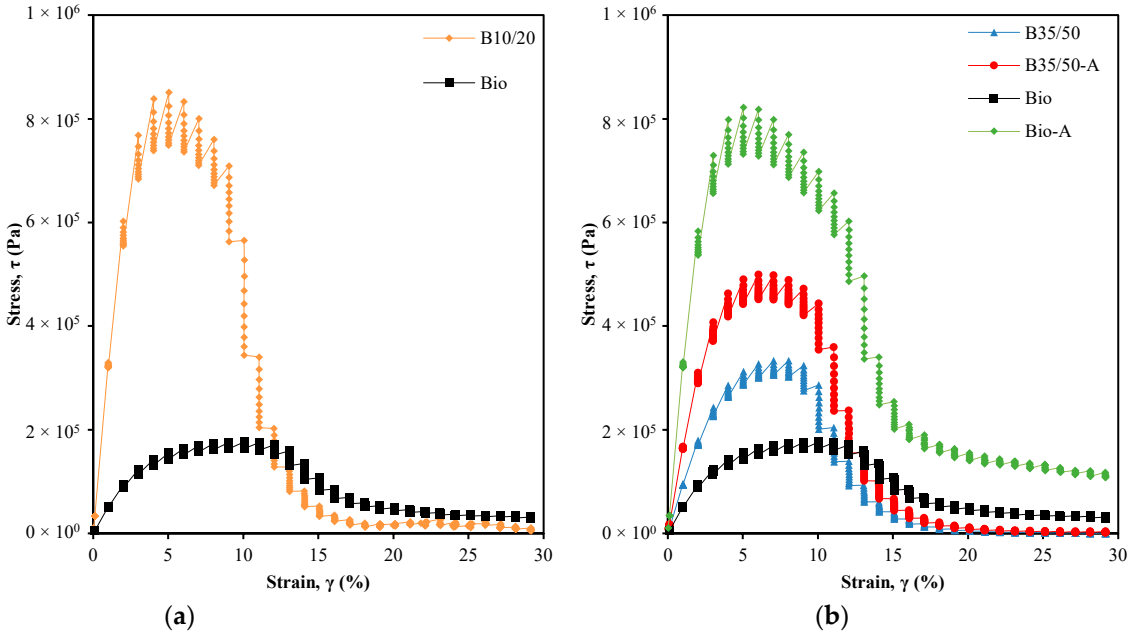

Figure 10. Shear stress evolution in LAS test: (**a**) B10/20 and Bio; (**b**) B35/50, B35/50-A, Bio and Bio-A.

The fatigue laws shown in Figure 11 estimate the number of cycles that the binders can be expected to resist before failure at different strain amplitudes. In Figure 11a, it is shown that Bio inherited the strain dependence (slope B—Equation (7)) of the base bitumen (B10/20); however, the fatigue resistance was much greater because the specimen's failure was attained at larger strains in the test. Thus, confirming the abovementioned differences in the stress evolution with applied strain, Figure 11b shows the significant decrease in the number of cycles to failure of Bio-A in comparison with the unaged state. Conversely, bitumen B35/50 had similar fatigue resistance before and after being exposed to the ageing treatment. Also, there was an increase in strain dependency in Bio-A, which means that the fatigue resistance decreased faster with the increase in the applied strain amplitude. The estimated fatigue resistance of Bio-A was only greater than that of B35/50-A at strain amplitudes smaller than 3.5%.

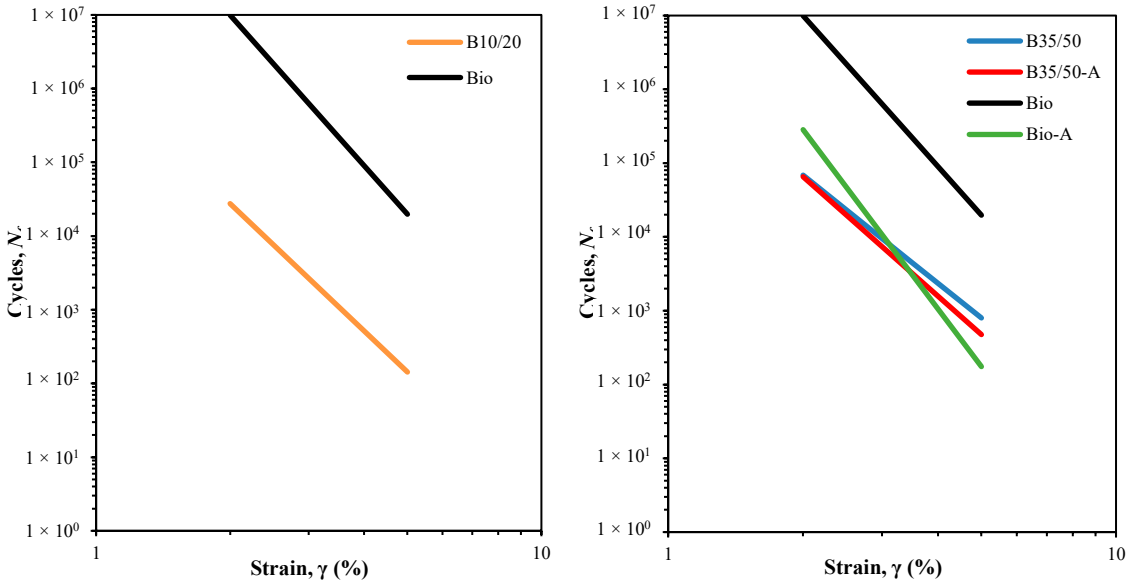

Figure 11. Fatigue law: (**a**) B10/20 and Bio; (**b**) B35/50, B35/50-A, Bio and Bio-A.

4.5. LVE Rheological-Based Performance Indicators

The performance of asphalt pavements in-service is highly affected by the bitumen's properties, especially its time–temperature-dependent response when loaded by traffic or deformed by temperature variations. However, traffic and climatic conditions vary widely; thus, extensive characterisations of materials' behaviour and the selection of adequate bitumens to attend to specific site conditions are required. In this study, the LVE rheological characterisation of the investigated materials covered the three regions of interest in bitumen rheological behaviour, i.e., the near-glassy region, the intermediate region and the terminal region, and some relevant indicators based on this characterisation are discussed in this section. Table 6 lists the ten indicators' values for the studied materials.

Table 6. LVE rheological-based performance indicators of bitumens and bio-bitumens.

Performance Indicator	B10/20	B35/50	B35/50-A	Bio	Bio-A
T_g (°C)	−12.9	−15.6	−17.7	<−30	−18.6
$\lvert G^* \rvert_g$ (Pa)	5.8×10^8	4.7×10^8	5.9×10^8	1.0×10^9 *	6.1×10^8
T_c (°C)	21.9	11.5	17.1	50.6	100.4
$\lvert G^* \rvert_c$ (Pa)	1.0×10^7	1.7×10^7	1.1×10^7	9.8×10^4	2.0×10^4
ΔT_{IR} (°C)	34.8	27.2	34.8	>80	119.1
R-value (Log (Pa))	1.75	1.43	1.74	4.00	4.48
T_{5MPa} (°C)	27.0	19.4	21.9	15.6	33.9
δ_{5MPa} (°)	51	54	50	34	34
T_{50kPa} (°C)	57.4	45.9	51.5	57.2	87.5
δ_{50kPa} (°)	72	75	71	47	41

* Not determined.

The transition between the near-glassy region and the intermediate region occurred at lower temperatures for the bio-bitumens in comparison with the paving-grade bitumens. Thus, the T_g of the unaged bio-bitumen (Bio) could not be exactly determined because it was lower than the lowest test temperature (−30 °C). For the paving-grade bitumens, the transition temperature was lower than for the softer bitumens. This temperature is important for the performance of asphalt pavements in very cold weather. Below T_g, the material accumulates more thermal stresses due to the reduced ability of molecular motion, which leads to eventual cracking [4].

Furthermore, T_g is not expected to vary (decrease/increase) significantly with increasing (oxidative) ageing, despite the chemical changes in bitumen [83]. With ageing, there is a decrease in the proportion of aromatics that have T_g close to that of the bitumen (around −20 °C) and an increase in "solid" type groups (resins and asphaltenes), which, according to some researchers [5,84], do not contribute significantly to the glass transition phenomenon. On the contrary, saturates exhibit a very low glass transition (around −70 °C), but their proportion in bitumen remains almost unchanged with ageing. Hence, Bio-A had a significantly higher T_g than Bio; however, the same did not happen for B35/50 and B35/50-A, which showed a slight decrease in T_g after the RTFOT treatment. Nevertheless, the studied paving-grade bitumens and bio-bitumens had an acceptable T_g for use in regions with mild winters, like in southern Europe.

Fatigue cracking is the main concern relative to performance at intermediate temperatures, at which bitumen behaves like a viscoelastic material, and ductility and flexibility are required to support traffic loading without premature cracking. To this purpose, the transition point between the predominant elastic state to a viscous-like state (T_c and $|G^*|_c$) and the amplitude range in modulus (ΔTIR) or temperature (*R-value*) from the near-glass transition point and the former transition point have been proposed as proxies of performance tests, such as ductility and fatigue tests [57]. The transition point is referred to as the crossover point because it corresponds to the point at which the G' and G'' values are equal (δ = 45°). Conventionally, the more elastic the material is, the higher the residual stresses due to the longer relaxation time and, consequently, the material is more susceptible to cracking. Thus, Jing et al. [61] reported that the relaxation properties worsened (longer times) with ageing as expected and that the ageing indexes calculated with the relaxation time and the crossover modulus had a strong linear correlation. Similarly, Elwardany et al. [58] stated that bitumens with ΔTIR greater than 50 °C had poor relaxation properties and cracking resistance. As shown in Table 6, the crossover points occurred at very different temperatures and shear moduli for the paving-grade bitumens and the bio-bitumens. For the paving-grade bitumens, the temperature was 11.5–21.9 °C and the modulus 10–17 MPa, while, for the bio-bitumens, the range values were 50.6–100.4 °C and 0.02–0.10 MPa. From this, it can be concluded that the intermediate region amplitudes (ΔTIR and *R*-value) were much greater for the bio-bitumens. As commented before in Section 4.2, it is possible that the bio-oil molecular groups interacted with the molecular groups of B10/20 to form larger, more polar colloid agglomerations that increased the elastic behaviour—but not the stiffness—over a wide temperature range, even when the bitumen was soft and easily flowable (above the softening point). Hence, the temperature and phase angle at which the critical stiffness of 5 MPa was met were lower for Bio than for the paving-grade bitumens. For Bio, the stiffness level was reached at a temperature much lower than the crossover temperature; hence, the low phase angle. However, except for the *R*-value, the LVE rheological indicators for the performance at intermediate temperatures of Bio were more affected by oxidative ageing than those of B35/50. The crossover temperature increased by approximately 50 °C for Bio and only 6 °C for B35/50.

Relative to the rheological indicator related to performance at high service temperatures, the stiffness level of 50 kPa was reached at a temperature in the range of 45.9–57.4 °C for paving-grade bitumens and 57.2–87.5 °C for bio-bitumens. Also, the phase angle values ranged from 71 to 75° for the former and 41 to 47° for the latter. Similarly, for the intermediate temperature indicators, the rheological behaviour of Bio was significantly less viscous in the high service temperature range, but it was highly affected by oxidative ageing. The critical temperature for rutting increased by 30 °C after RTFOT, whereas it only changed by 6 °C for B35/50.

The radar chart type is used in Figure 12 to show a comparison of the relationship between the rheological indicators and the performance tests for the paving-grade bitumens and the bio-bitumens. Four rheological indicators (T_g, T_c, $T_{5\text{MPa}}$ and $T_{50\text{kPa}}$) and two performance test variables ($N_f{}^{\gamma\,=3.5\%}$ and $J_{nr\ 2\text{kPa}}$) are plotted. In this situation, T_c and T_{5MPa} are compared to $N_f{}^{\gamma\,=3.5\%}$ and $T_{50\text{kPa}}$ is compared to $J_{nr\ 2\text{kPa}}$. Although there

was no test performed on thermal cracking resistance, T_g was plotted to give an overall view of the materials' glassy transition. The axes' properties (min–max amplitude and increase/decrease direction) were defined so that for each axis, the longer the distance from the chart centre, the better the expected performance. Therefore, the inside area was expected to shrink when the material deteriorated. For the paving-grade bitumens, the rheological indicators and performance tests showed the expected variation, i.e., fatigue resistance was greater with smaller T_c and $T_{5\text{MPa}}$ values and non-recoverable compliance was smaller with higher $T_{50\text{kPa}}$ values. However, while for fatigue performance, a small variation in the rheological indicators corresponded to a small variation in fatigue resistance, non-recoverable compliance had a large variation with a small change in $T_{50\text{kPa}}$. In line with this, B35/50 showed high resistance to oxidative ageing, except in the multiple stress creep and recovery test.

However, the relationship between the rheological indicators and the performance test results was not the same for paving-grade and bio-bitumens. For example, the T_c of Bio was higher than that of paving-grade bitumens, but the fatigue resistance was much greater. The rheological indicator values could not be directly compared because, as stated by Garcia Cucalon et al. [57], the same change in the rheological properties (e.g., decrease in the phase angle) can have different effects on performance and durability, depending on the cause (e.g., ageing vs. polymer modification). The bio-oil had a substantial effect on the rheology of the bitumen, which was likely related to the interaction of the bio-oil and the bitumen's molecules. Also, the rheological characterisation in the LVE region of structured bitumens (e.g., gel structure or modified bitumens) may be less correlated with flexibility and durability. Nevertheless, these indicators are useful in ageing resistance studies. Thus, the significant change in the rheological indicators matched the decrease in the fatigue resistance of the aged bio-binder. The non-recoverable compliance did not change because it was already very low for the unaged material and it improves with ageing.

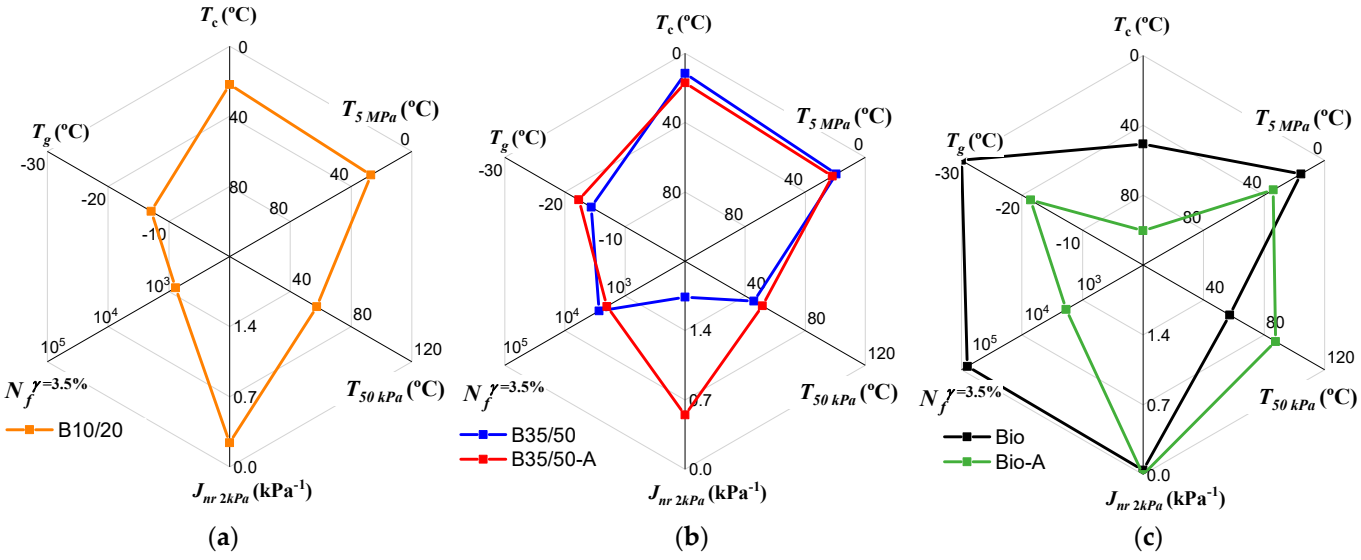

Figure 12. Comparison of LVE indicators and performance tests: (**a**) B10/20; (**b**) B35/50 and B35/50-A; (**c**) Bio and Bio-A.

5. Conclusions

This study aimed to investigate the effect of incorporating a liquified wood heavy fraction (bio-oil) in bitumen on its rheological behaviour, intermediate- and high-temperature performance, and evolution with oxidative ageing. The biomass used was a waste wood comprising pinewood residues resulting from systematic cleaning interventions of forested areas or -post-fire situations, and it was processed using an innovative thermochemical liquefaction process. The results of the bio-bitumen (15% bio-oil) were compared with those

of the base bitumen (blended with the bio-oil) and bitumen with the same penetration grade as the bio-bitumen.

The following conclusions are drawn:

- The effect of bio-oil on the needle penetration test result at 25 °C was significantly larger than that predicted using the conventional blending rule for different bitumens (EN 13108-1). However, this blending rule can be used for estimating the softening point.
- The bio-bitumen was not a thermo-rheologically simple material, meaning that there was no equivalence of time and temperature conditions in the dynamic rheological measurements. In comparison with the base bitumen (B10/20), the bio-oil changed the shape of the Black curve, decreased the phase angle (greater elastic response) and yielded discontinuities between measurements obtained at consecutive temperatures. These changes were similar to those reported in the literature [69,72] of more structured bitumens induced by natural functional groups or polymer modification. Also, the near-glass transition temperature (T at G″ max) of bio-bitumen was lower than that of the other bitumens tested, which is an indicator of superior performance in very cold weather.
- The bio-oil significantly improved the resistance to fatigue and permanent deformation accumulation of the base bitumen. Upon cyclic loading, the bio-bitumen was equally able to hold larger strains before failure at the intermediate test temperature (20 °C) and had greater elastic recovery at the high test temperature (60 °C). The elastic recovery value reached 64.7% at 3.2 kPa and non-recoverable compliance decreased to 0.044 kPa^{-1}. Thus, the deformation recovery occurred very quickly after the stress removal because the elastic component in the rheological behaviour of bio-bitumen is very strong, which is only commonly found in highly polymer-modified bitumen.
- The bio-bitumen was more sensitive to oxidative ageing than the reference bitumen (B35/50). In detail, the retained penetration was 31%, the increase in the softening point was 27.1 °C, the rheological behaviour was elastic (δ < 45 °C) up to 64 °C, the elastic recovery at 3.2 kPa increased by 29.7% and, in the LAS test, the strain at peak stress decreased by 5%.
- The LVE rheological indicators proposed in the literature showed a similar trend of variation with oxidative ageing for the bio-bitumens and paving-grade bitumens. However, the relationship between the performance test results and LVE rheological indicators was not the same in the two binders, i.e., for similar indicator values in both materials, the test performance could be significantly different.

Although the results obtained in this research only apply to the studied bio-oil and bitumens, it shows once more that waste-wood-derived bio-oils are a sustainable solution to partially replace bitumen for road paving applications. However, bio-oil's chemical and physical properties change with the biomass origin and processing technique, which affects the interactions with the bitumen in the blending process. The produced bio-bitumen showed an interesting predominant elastic behaviour at high in-service temperatures (50 °C), without affecting fatigue performance, but the oxidative ageing resistance was weak. Following studies are intended to investigate in greater detail the chemical composition of this bio-oil and the bio-bitumen to understand the oxidative ageing mechanisms and the origin of the strong elastic response.

Author Contributions: Conceptualization, M.S.-d.-C., R.M. and J.N.; methodology, M.S.-d.-C., R.M. and J.N.; validation, M.S.-d.-C. and R.M.; formal analysis, V.C., M.S.-d.-C. and R.M.; investigation, V.C. and M.S.-d.-C.; resources, M.S.-d.-C., C.A., V.C, R.G.d.S. and J.B.; writing—original draft preparation, V.C., M.S.-d.-C. and R.M.; writing—review and editing, M.S.-d.-C., R.M. and J.N.; supervision, M.S.-d.-C., R.M. and J.N.; project administration, M.S.-d.-C. and J.N. All authors have read and agreed to the published version of the manuscript.

Funding: This paper was developed within the scope of project no. 047061, "BioRoadPAV—New Bio-Binders for Application on Road Pavements", co-financed by the Competitiveness and Inter-

nationalization Operational Program (PO CI) and the Lisbon Regional Operational Program (PO LISBOA) through the Portugal 2020 Program and European Regional Development Fund (FEDER). The authors are grateful for the Foundation for Science and Technology's support through funding FCT-UIDB/04625/2020 given to research unit CERIS (Center for Civil Engineering Research and Innovation for Sustainability) and FCT-UIDB/04028/2020 to CERENA (Center for Natural Resources and Environment).

Institutional Review Board Statement: Not applicable.

Informed Consent Statement: Not applicable.

Data Availability Statement: Data are contained within the article.

Acknowledgments: The authors gratefully acknowledge Respol Resinas S.A. for providing the bio-oil samples and Diogo Gonçalves, Researcher at CERENA, for the laboratory characterisation of the liquified wood heavy fraction.

Conflicts of Interest: Author Carlos Alpiarça was employed by the company LUSASFAL—Derivados Asfálticos de Portugal, S.A. The remaining authors declare that the research was conducted in the absence of any commercial or financial relationships that could be construed as a potential conflict of interest.

References

1. Malhotra, S.K.; White, H.; Dela Cruz, N.A.O.; Saran, A.; Eyers, J.; John, D.; Beveridge, E.; Blöndal, N. Studies of the Effectiveness of Transport Sector Interventions in Low- and Middle-income Countries: An Evidence and Gap Map. *Campbell Syst. Rev.* **2021**, *17*, e1203. [CrossRef]
2. Xing, J.; Leard, B.; Li, S. What Does an Electric Vehicle Replace? *J. Environ. Econ. Manag.* **2021**, *107*, 102432. [CrossRef]
3. Vilchez, J.J.G. The Impact of Electric Cars on Oil Demand and Greenhouse Gas Emissions in Key Markets. Ph.D. Thesis, Karlsruher Institut für Technologie, Karlsruhe, Germany, 2018.
4. Hunter, R.N.; Shelf, A.; Read, J. *The Shell Bitumen Handbook*, 6th ed.; ICE Publishing: London, UK, 2015.
5. Lesueur, D. The Colloidal Structure of Bitumen: Consequences on the Rheology and on the Mechanisms of Bitumen Modification. *Adv. Colloid Interface Sci.* **2009**, *145*, 42–82. [CrossRef] [PubMed]
6. Petersen, J. *A Review of the Fundamentals of Asphalt Oxidation: Chemical, Physicochemical, Physical Property, and Durability Relationships*; Transportation Research Board: Washington, DC, USA, 2009; p. 78.
7. Antunes, V.; Moreno, F.; Rubio-Gámez, M.; Freire, A.C.; Neves, J. Assessing RAP Multi-Recycling Capacity by the Characterization of Recovered Bitumen Using DSR. *Sustainability* **2022**, *14*, 10171. [CrossRef]
8. Zhang, Z.; Fang, Y.; Yang, J.; Li, X. A Comprehensive Review of Bio-Oil, Bio-Binder and Bio-Asphalt Materials: Their Source, Composition, Preparation and Performance. *J. Traffic Transp. Eng.* **2022**, *9*, 151–166. [CrossRef]
9. Yu, H.; Xu, Y.; Havener, K.; Zhang, M.; Zhang, L.; Wu, W.; Huang, K. Temperature-Controlled Selectivity of Hydrogenation and Hydrodeoxygenation of Biomass by Superhydrophilic Nitrogen/Oxygen Co-Doped Porous Carbon Nanosphere Supported Pd Nanoparticles. *Small* **2022**, *18*, 2106893. [CrossRef] [PubMed]
10. Toor, S.S.; Rosendahl, L.; Rudolf, A. Hydrothermal Liquefaction of Biomass: A Review of Subcritical Water Technologies. *Energy* **2011**, *36*, 2328–2342. [CrossRef]
11. Demirbas, A. Combustion Characteristics of Different Biomass Fuels. *Prog. Energy Combust. Sci.* **2004**, *30*, 219–230. [CrossRef]
12. Espinosa, L.V.; Gadler, F.; Mota, R.V.; Vasconcelos, K.L.; Bernucci, L.L.B. Comparison Between Rheological Behavior of a Neat Asphalt Binder and a Bio-Binder from Renewable Source. In *Proceedings of the RILEM International Symposium on Bituminous Materials*; Di Benedetto, H., Baaj, H., Chailleux, E., Tebaldi, G., Sauzéat, C., Mangiafico, S., Eds.; RILEM Bookseries; Springer International Publishing: Cham, Switzerland, 2022; Volume 27, pp. 443–448, ISBN 978-3-030-46454-7.
13. Pérez, I.P.; Rodríguez Pasandín, A.M.; Pais, J.C.; Alves Pereira, P.A. Use of Lignin Biopolymer from Industrial Waste as Bitumen Extender for Asphalt Mixtures. *J. Clean. Prod.* **2019**, *220*, 87–98. [CrossRef]
14. Park, K.-B.; Kim, J.-S.; Pahlavan, F.; Fini, E.H. Biomass Waste to Produce Phenolic Compounds as Antiaging Additives for Asphalt. *ACS Sustain. Chem. Eng.* **2022**, *10*, 3892–3908. [CrossRef]
15. Guarin, A.; Khan, A.; Butt, A.A.; Birgisson, B.; Kringos, N. An Extensive Laboratory Investigation of the Use of Bio-Oil Modified Bitumen in Road Construction. *Constr. Build. Mater.* **2016**, *106*, 133–139. [CrossRef]
16. Somé, S.C.; Pavoine, A.; Chailleux, E. Evaluation of the Potential Use of Waste Sunflower and Rapeseed Oils-Modified Natural Bitumen as Binders for Asphalt Pavement Design. *Int. J. Pavement Res. Technol.* **2016**, *9*, 368–375. [CrossRef]
17. Uz, V.E.; Gökalp, İ. Sustainable Recovery of Waste Vegetable Cooking Oil and Aged Bitumen: Optimized Modification for Short and Long Term Aging Cases. *Waste Manag.* **2020**, *110*, 1–9. [CrossRef]
18. Ingrassia, L.P.; Lu, X.; Ferrotti, G.; Canestrari, F. Chemical, Morphological and Rheological Characterization of Bitumen Partially Replaced with Wood Bio-Oil: Towards More Sustainable Materials in Road Pavements. *J. Traffic Transp. Eng.* **2020**, *7*, 192–204. [CrossRef]

19. Gong, M.; Yang, J.; Zhang, J.; Zhu, H.; Tong, T. Physical–Chemical Properties of Aged Asphalt Rejuvenated by Bio-Oil Derived from Biodiesel Residue. *Constr. Build. Mater.* **2016**, *105*, 35–45. [CrossRef]
20. Azahar, W.N.A.W.; Jaya, R.P.; Hainin, M.R.; Bujang, M.; Ngadi, N. Chemical Modification of Waste Cooking Oil to Improve the Physical and Rheological Properties of Asphalt Binder. *Constr. Build. Mater.* **2016**, *126*, 218–226. [CrossRef]
21. Zargar, M.; Ahmadinia, E.; Asli, H.; Karim, M.R. Investigation of the Possibility of Using Waste Cooking Oil as a Rejuvenating Agent for Aged Bitumen. *J. Hazard. Mater.* **2012**, *233–234*, 254–258. [CrossRef]
22. Fernandes, S.; Peralta, J.; Oliveira, J.; Williams, R.; Silva, H. Improving Asphalt Mixture Performance by Partially Replacing Bitumen with Waste Motor Oil and Elastomer Modifiers. *Appl. Sci.* **2017**, *7*, 794. [CrossRef]
23. Wang, H.; Ma, Z.; Chen, X.; Mohd Hasan, M.R. Preparation Process of Bio-Oil and Bio-Asphalt, Their Performance, and the Application of Bio-Asphalt: A Comprehensive Review. *J. Traffic Transp. Eng.* **2020**, *7*, 137–151. [CrossRef]
24. Weir, A.; Jiménez Del Barco Carrión, A.; Queffélec, C.; Bujoli, B.; Chailleux, E.; Uguna, C.N.; Snape, C.; Airey, G. Renewable Binders from Waste Biomass for Road Construction: A Review on Thermochemical Conversion Technologies and Current Developments. *Constr. Build. Mater.* **2022**, *330*, 127076. [CrossRef]
25. Ingrassia, L.P.; Canestrari, F. VECD Analysis to Investigate the Performance of Long-Term Aged Bio-Asphalt Mixtures Compared to Conventional Asphalt Mixtures. *Road Mater. Pavement Des.* **2022**, *23*, 2697–2712. [CrossRef]
26. McKendry, P. Energy Production from Biomass (Part 1): Overview of Biomass. *Bioresour. Technol.* **2002**, *83*, 37–46. [CrossRef] [PubMed]
27. Zhang, X.; Brown, R.C. Chapter 1: Introduction to Thermochemical Processing of Biomass into Fuels, Chemicals, and Power. In *Thermochemical Processing of Biomass: Conversion into Fuels, Chemicals and Power*; John Wiley & Sons: Hoboken, NJ, USA, 2019.
28. Elliott, D.C.; Biller, P.; Ross, A.B.; Schmidt, A.J.; Jones, S.B. Hydrothermal Liquefaction of Biomass: Developments from Batch to Continuous Process. *Bioresour. Technol.* **2015**, *178*, 147–156. [CrossRef] [PubMed]
29. Machado, H.; Cristino, A.F.; Orišková, S.; Galhano Dos Santos, R. Bio-Oil: The Next-Generation Source of Chemicals. *Reactions* **2022**, *3*, 118–137. [CrossRef]
30. Raouf, M.A.; Williams, C.R. General Rheological Properties of Fractionated Switchgrass Bio-Oil as a Pavement Material. *Road Mater. Pavement Des.* **2010**, *11*, 325–353. [CrossRef]
31. Ameri, A.; Haghshenas, H.F.; Fini, E.H. Future Directions for Applications of Bio-Oils in the Asphalt Industry: A Step to Sequester Carbon in Roadway Infrastructure. *Energy Fuels* **2023**, *37*, 4791–4815. [CrossRef]
32. Zhang, X.; Zhang, K.; Wu, C.; Liu, K.; Jiang, K. Preparation of Bio-Oil and Its Application in Asphalt Modification and Rejuvenation: A Review of the Properties, Practical Application and Life Cycle Assessment. *Constr. Build. Mater.* **2020**, *262*, 120528. [CrossRef]
33. *Eurobitume The Eurobitume Life Cycle Inventory for Bitumen, Version 3.1*; European Bitumen Association: Brussels, Belgium, 2020.
34. Samieadel, A.; Schimmel, K.; Fini, E.H. Comparative Life Cycle Assessment (LCA) of Bio-Modified Binder and Conventional Asphalt Binder. *Clean Technol. Environ. Policy* **2018**, *20*, 191–200. [CrossRef]
35. Grilli, A.; Iori, L.; Porot, L. Effect of Bio-Based Additives on Bitumen Properties. *Road Mater. Pavement Des.* **2019**, *20*, 1864–1879. [CrossRef]
36. Kalampokis, S.; Papamoschou, M.; Kalama, D.M.; Pappa, C.P.; Manthos, E.; Triantafyllidis, K.S. Investigation of the Characteristic Properties of Lignin-Modified Bitumen. *CivilEng* **2022**, *3*, 734–747. [CrossRef]
37. Pérez, I.; Pasandín, A.R.; Pais, J.C.; Pereira, P.A.A. Feasibility of Using a Lignin-Containing Waste in Asphalt Binders. *Waste Biomass Valor* **2020**, *11*, 3021–3034. [CrossRef]
38. Yu, J.; Guo, Y.; Peng, L.; Guo, F.; Yu, H. Rejuvenating Effect of Soft Bitumen, Liquid Surfactant, and Bio-Rejuvenator on Artificial Aged Asphalt. *Constr. Build. Mater.* **2020**, *254*, 119336. [CrossRef]
39. Adesina, P.A.; Dahunsi, B.I. Blended Waste Utilization in Road Construction: Physical Characteristics of Bitumen Modified with Waste Cooking Oil and High-Density Polyethylene. *Int. J. Pavement Res. Technol.* **2021**, *14*, 98–104. [CrossRef]
40. Sun, Z.; Yi, J.; Huang, Y.; Feng, D.; Guo, C. Properties of Asphalt Binder Modified by Bio-Oil Derived from Waste Cooking Oil. *Constr. Build. Mater.* **2016**, *102 Pt 1*, 496–504. [CrossRef]
41. Goncalves, D.; Orišková, S.; Matos, S.; Machado, H.; Vieira, S.; Bastos, D.; Gaspar, D.; Paiva, R.; Bordado, J.C.; Rodrigues, A.; et al. Thermochemical Liquefaction as a Cleaner and Efficient Route for Valuing Pinewood Residues from Forest Fires. *Molecules* **2021**, *26*, 7156. [CrossRef]
42. Neves, J.; da Costa, M.S.; Galhano, R.; Bordado, J.; Santos, L.D.P.; Freire, A.C.; Fontul, S.; Alpiarça, C.; Freitas, J.; Cordeiro, V. Research on Innovative Biobinders for Sustainable Road Pavements The BioRoadPAV Project. *Transp. Res. Procedia* **2023**, *72*, 399–406. [CrossRef]
43. *EN 12607-1*; Bitumen and Bituminous Binders—Determination of the Resistance to Hardening under the Influence of Heat and Air—Part 1: RTFOT Method. European Committee for Standardization: Brussels, Belgium, 2014.
44. *CEN EN 1426:2015*; Bitumen and Bituminous Binders—Determination of Needle Penetration. European Committee for Standardization: Brussels, Belgium, 2015.
45. *CEN EN 1427:2015*; Bitumen and Bituminous Binders—Determination of the Softening Point: Ring and Ball Method. European Committee for Standardization: Brussels, Belgium, 2015.
46. *CEN EN 14770:2012*; Bitumen and Bituminous Binders—Determination of Complex Shear Modulus and Phase Angle—Dynamic Shear Rheometer (DSR). European Committee for Standardization: Brussels, Belgium, 2012.

47. *CEN EN 16659:2015*; Bitumen and Bituminous Binders: Multiple Stress and Recovery Test (MSCRT). European Committee for Standardization: Brussels, Belgium, 2015.
48. *AASHTO TP 391-20*; Estimating Fatigue Resistance of Asphalt Binders Using the Linear Amplitude Sweep. American Association of State Highway and Transportation Officials: Washington, DC, USA, 2020.
49. Carl, C.; Lopes, P.; Sá da Costa, M.; Canon Falla, G.; Leischner, S.; Micaelo, R. Comparative Study of the Effect of Long-Term Ageing on the Behaviour of Bitumen and Mastics with Mineral Fillers. *Constr. Build. Mater.* **2019**, *225*, 76–89. [CrossRef]
50. Safaei, F.; Castorena, C. Material Nonlinearity in Asphalt Binder Fatigue Testing and Analysis. *Mater. Des.* **2017**, *133*, 376–389. [CrossRef]
51. Johnson, C.M. Estimating Asphalt Binder Fatigue Resistance Using an Accelerated Test Method. Ph.D. Thesis, University of Madison-Wisconsin, Madison, WI, USA, 2010.
52. Petersen, J.C.; Robertson, R.E.; Branthaver, J.; Harnsberger, P.; Duvall, J.J.; Kim, S.; Anderson, D.A.; Christiansen, D.W.; Bahia, H.U.; Dongre, R.; et al. *SHRP-A-370. Binder Characterization and Evaluation. Volume 4*; Strategic Highway Research Program, National Research Council: Washington, DC, USA, 1994; Volume SHRP-A-370, ISBN 978-0-309-05806-3.
53. *C-SHRP SUPERPAVE Binder Specification and Test Methods*; Canadian Strategic Highway Research Program (C-SHRP), Transportation Association of Canada: Ottawa, Canada, 1995; Volume Technical brief #9, ISBN 1-55187-018-5.
54. Subhy, A. Advanced Analytical Techniques in Fatigue and Rutting Related Characterisations of Modified Bitumen: Literature Review. *Constr. Build. Mater.* **2017**, *156*, 28–45. [CrossRef]
55. Bahia, H.U.; Hanson, D.L.; Zeng, M.; Zhai, H.; Khatri, M.A.; Anderson, R.M. *Characterization of Modified Asphalt Binders in Superpave Mix Design*; Transportation Research Board: Washington, DC, USA, 2001.
56. Durand, G.; Robert, M.; Morin, E. Which Are the Best Rheological Criteria for Characterization of PMB? In Proceedings of the 7th Eurasphalt & Eurobitume Congress, Madrid, Spain, 15–17 June 2021.
57. Garcia Cucalon, L.; Kaseer, F.; Arámbula-Mercado, E.; Epps Martin, A.; Morian, N.; Pournoman, S.; Hajj, E. The Crossover Temperature: Significance and Application towards Engineering Balanced Recycled Binder Blends. *Road Mater. Pavement Des.* **2019**, *20*, 1391–1412. [CrossRef]
58. Elwardany, M.D.; Planche, J.-P.; Adams, J.J. Determination of Binder Glass Transition and Crossover Temperatures Using 4-Mm Plates on a Dynamic Shear Rheometer. *Transp. Res. Rec.* **2019**, *2673*, 247–260. [CrossRef]
59. Lei, Z.; Bahia, H.; Yi-qiu, T. Effect of Bio-Based and Refined Waste Oil Modifiers on Low Temperature Performance of Asphalt Binders. *Constr. Build. Mater.* **2015**, *86*, 95–100. [CrossRef]
60. Farrar, M.J.; Turner, T.F.; Planche, J.-P.; Schabron, J.F.; Harnsberger, P.M. Evolution of the Crossover Modulus with Oxidative Aging: Method to Estimate Change in Viscoelastic Properties of Asphalt Binder with Time and Depth on the Road. *Transp. Res. Rec.* **2013**, *2370*, 76–83. [CrossRef]
61. Jing, R.; Varveri, A.; Liu, X.; Scarpas, A.; Erkens, S. Rheological, Fatigue and Relaxation Properties of Aged Bitumen. *Int. J. Pavement Eng.* **2020**, *21*, 1024–1033. [CrossRef]
62. *EN 13108-1:2016*; Bituminous Mixtures. Materials Specifications. Part 1: Asphalt Concrete. European Committee for Standardization: Brussels, Belgium, 2016.
63. Airey, G.D. Rheological Properties of Styrene Butadiene Styrene Polymer Modified Road Bitumens☆. *Fuel* **2003**, *82*, 1709–1719. [CrossRef]
64. *EN 12591:2009*; Bitumen and Bituminous Binders—Specifications for Paving Grade Bitumens. European Committee for Standardization: Brussels, Belgium, 2009.
65. *EN 13924-1:2015*; Bitumen and Bituminous Binders—Specification Framework for Special Paving Grade Bitumen—Part 1: Hard Paving Grade Bitumens. European Committee for Standardization: Brussels, Belgium, 2015.
66. Airey, G.D. Use of Black Diagrams to Identify Inconsistencies in Rheological Data. *Road Mater. Pavement Des.* **2002**, *3*, 403–424. [CrossRef]
67. Petersen, J.C. *Binder Characterization and Evaluation*; Strategic Highway Research Program, National Research Council: Washington, DC, USA, 1994; ISBN 978-0-309-05809-4.
68. Soenen, H.; Lu, X.; Robertus, C.; Carbonneau, X.; Durand, G. Durability Parameters Evaluated on Binders Recovered from Various Field Sites in Europe. In Proceedings of the 7th Eurasphalt & Eurobitume Congress, Madrid, Spain, 15–17 June 2021.
69. Eckmann, B.; Largeaud, S.; Van Rooijen, R.; Planche, L.; Farrar, M.; Planche, J.-P. New Bitumen Performance Indicators—A Feasibility Study. In Proceedings of the 6th Eurasphalt & Eurobitume Congress, Prague, Czech Republic, 1–3 June 2016.
70. Huang, S.-C.; Zeng, M. Characterization of Aging Effect on Rheological Properties of Asphalt-Filler Systems. *Int. J. Pavement Eng.* **2007**, *8*, 213–223. [CrossRef]
71. Airey, G.D. Factors Affecting the Rheology of Polymer Modified Bitumen (PMB). In *Polymer Modified Bitumen*; Woodhead Publishing Series in Civil and Structural Engineering; Elsevier: Amsterdam, The Netherlands, 2011; pp. 238–263, ISBN 978-0-85709-048-5.
72. Hajikarimi, P.; Fakhari Tehrani, F.; Moghadas Nejad, F.; Absi, J.; Rahi, M.; Khodaii, A.; Petit, C. Mechanical Behavior of Polymer-Modified Bituminous Mastics. I: Experimental Approach. *J. Mater. Civ. Eng.* **2019**, *31*, 04018337. [CrossRef]
73. Büchner, J.; Sigwarth, T.; Wistuba, M. *Testing Conditions for Asphalt Binder Testing Using Dynamic Shear Rheometer with 4 Mm Diameter Parallel Plate Geometry*; Braunschweig Pavement Engineering Centre (ISBS): Braunschweig, Germany, 2021. [CrossRef]

74. Farrar, M.; Sui, C.; Salmans, S.; Qin, Q. *Determining the Low-Temperature Rheological Properties of Asphalt Binder Using a Dynamic Shear Rheometer (DSR)*; Western Research Institute: Laramie, WY, USA, 2015.
75. Batista, F.A.; Hofko, B.; Visscher, J.D.; Tanghe, T.; da Costa, M.S. Towards Improved Correlations between Bitumen Properties and Rutting Resistance of Bituminous Mixtures—FunDBitS Literature Review. *IOP Conf. Ser. Mater. Sci. Eng.* **2017**, *236*, 012001. [CrossRef]
76. Ribeiro, T.; Freire, A.C.; Sá-da-Costa, M.; Canejo, J.; Cordeiro, V.; Micaelo, R. Investigating Asphalt Self-Healing with Colorless Binder and Pigmented Rejuvenator. *Sustainability* **2023**, *15*, 4556. [CrossRef]
77. Porot, L.; Zhu, J.; Wang, D.; Cannone Falchetto, A. Multiple Stress Creep Recovery Test to Differentiate Polymer Modified Bitumen at High Temperature. *J. Test. Eval.* **2022**, *51*, 20220306. [CrossRef]
78. Baumgardner, G. *Multiple Stress Creep and Recovery (MSCR) Implementation and Transition*; University of Nevada: Reno, NV, USA, 2020.
79. *AASHTO M 332-14*; Performance-Graded Asphalt Binder Using Multiple Stress Creep Recovery (MSCR) Test. American Association of State Highway and Transportation Officials: Washington, DC, USA, 2014.
80. Salim, R.; Gundla, A.; Underwood, B.S.; Kaloush, K.E. Effect of MSCR Percent Recovery on Performance of Polymer Modified Asphalt Mixtures. *Transp. Res. Rec.* **2019**, *2673*, 308–319. [CrossRef]
81. Pereira, A.; Micaelo, R.; Quaresma, L.; Cidade, M.T. Evaluation of Different Methods for the Estimation of the Bitumen Fatigue Life with DSR Testing. In *8th RILEM International Symposium on Testing and Characterization of Sustainable and Innovative Bituminous Materials*; Canestrari, F., Partl, M.N., Eds.; Springer Netherlands: Dordrecht, The Netherlands, 2016; Volume 11, pp. 1017–1028, ISBN 978-94-017-7341-6.
82. Micaelo, R.; Botella, R.; Pérez-Jiménez, F.; Sá da Costa, M. Analysis of the Ageing Effect on the Cyclic Tension–Compression Loading Behaviour of Bitumen and Mastics. *Constr. Build. Mater.* **2020**, *243*, 118275. [CrossRef]
83. Sá da Costa, M.; Farcas, F.; Santos, L.F.; Eusébio, M.I.; Diogo, A.C. Chemical and Thermal Characterization of Road Bitumen Ageing. *Mater. Sci. Forum* **2010**, *636–637*, 273–279. [CrossRef]
84. Kriz, P.; Stastna, J.; Zanzotto, L. Glass Transition and Phase Stability in Asphalt Binders. *Road Mater. Pavement Des.* **2008**, *9* (Suppl. S1), 37–65. [CrossRef]